Energy, Mines and Resources Canada
Énergie, Mines et Ressources Canada

CANMET

Canada Centre for Mineral and Energy Technology

Centre canadien de la technologie des minéraux et de l'énergie

A PRELIMINARY STABILITY ASSESSMENT OF C-102-23 STOPE OF THE NIOBEC MINE UNDER GRAVITATIONAL LOADING

Y.S. YU, S. VONGPAISAL, N.A. TOEWS AND A.S. WONG
Rock Mechanics Laboratory

July 1986

This document is a [illegible] preliminary [illegible] and does not [illegible] purposes. It does not [illegible] a final expression of [illegible] of the Canada Centre for Mineral and Energy Technology (CANMET)

Ce document est un rapport [illegible] et intégré [illegible] de [illegible] de communication [illegible] de [illegible] de [illegible] et de l'énergie (CANMET)

MINERAL AND ENERGY TECHNOLOGY
MINING RESEARCH LABORATORIES
DIVISION REPORT M&ET/MRL 86-97(TR)

MICROMEDIA

A PRELIMINARY STABILITY ASSESSMENT OF C-102-23 STOPE OF THE NIOBEC MINE UNDER GRAVITATIONAL LOADING

by

Y.S. Yu*, S. Vongpaisal*, N.A. Toews* and A.S. Wong**

ABSTRACT

The stability of C-102-23 stope and its adjacent areas, in Zone 1 of the upper level, were analyzed using the three-dimensional finite element technique.

In this preliminary study the rock mass was assumed to be homogeneous, linearly elastic and isotropic, and subjected to gravitational loading. Site specific field stress and rock property data were not available at the time the simulation was made.

The results indicate that a large tensile stress zone occurs in the roof of C-102-23 stope. It extends vertically 10 metres into the roof at the centre of the span and horizontally more than 10m towards both the hanging and foot walls. Small tensile stress zones occur along almost the entire height of T-102-21 pillar. Local instabilities in the roof and around the pillars are anticipated.

Assuming values of 2 MPa and 40° for cohesion and angle of internal friction respectively, the local factors of safety in terms of Drucker/Prager yield criterion were evaluated. All calculated factors of safety were greater than 1.5. The occurrence of shear failure in the roof or pillars is not anticipated. If failures occur, they will be tension failures.

* Research Scientists, ** Physical Scientist, Mining Research Laboratories, CANMET, Energy, Mines and Resources Canada, Ottawa.

Key words: Niobec Mine, stability, stress analysis, finite element, three-dimensional

ÉVALUATION PRÉLIMINAIRE DE LA STABILITÉ DU CHANTIER C-102-23 DE LA MINE NIOBEC SOUS DES CHARGES GRAVITATIONNELLES

par

Y.S. Yu*, S. Vongpaisal*, N.A. Toews* et A.S. Wong**

RÉSUMÉ

On a étudié la stabilité du chantier C-102-23 et de ses sections adjacentes, dans la Zone 1 du niveau supérieur, à l'aide de la technique de l'élément fini tri-dimensionnelle.

Au cours de cette étude préliminaire, on a supposé que la masse rocheuse était homogène, d'une élasticité linéaire et isotropique, et soumise à des charges gravitationnelles. La contrainte naturelle spécifique du terrain et les données sur la propriété des roches n'étaient pas disponibles lors de cette simulation.

Les résultats d'essais ont indiqué qu'une grande zone d'effort de traction se produit dans le toit du chantier C-102-23. Cette zone s'étend verticalement sur une longueur de 10 mètres dans le toit au centre de la travée et horizontalement sur plus de 10 mètres vers le toit et les parois. De petites zones d'effort de traction se produisent sur presque toute la hauteur du pilier T-102-21. On prévoit donc des instabilités locales dans le toit et autour des piliers.

Les facteurs locaux de sécurité ont été évalués selon le critère d'élasticité Drucker/ Prager, en supposant pour la cohésion et l'angle de friction interne des valeurs de 2 MPa et de 40° respectivement. Tous les facteurs de sécurité calculés étaient plus élevés que 1,5. On ne prévoit pas la possibilité d'une rupture de cisaillement dans toit ou les piliers. Enfin, si des ruptures se produisent, ce seront des ruptures de tension.

* Chercheurs scientifiques, ** Physicien, Laboratoires de recherche minière, CANMET, Énergie, Mines et Ressources Canada, Ottawa.

Mots-clés: Mine Niobec, stabilité, analyse de traction, élément fini, tri-dimensionnel

CONTENTS

	page
ABSTRACT	i
RÉSUME	ii
1.0 INTRODUCTION	1
2.0 THE NIOBEC MINE	1
2.1 Geological Background	1
2.2 General Mining Conditions	3
2.3 Mine Layout	6
2.4 3-D Niobec Mine Model	9
2.5 Computer Program	14
2.6 Material Properties of Mine Rocks	14
2.7 In Situ Stresses	14
3.0 RESULTS	15
3.1 Stress Distributions	16
3.2 Safety Factor	16
3.3 Displacements	23
4.0 CONCLUSIONS AND RECOMMENDATIONS	23
5.0 ACKNOWLEDGEMENTS	33
6.0 REFERENCES	33

FIGURES

1. Regional geology of Niobec Mine 2
2. A typical cross sectional view of Niobec Mine 4
3. A typical open stope layout 5
4. Plan view of the Mine at Level 300 7
5. Longitudinal section at 150 + 50N 8
6. Isometric view of the Mine model 10
7a. The finite element discretization for section x = 106.68m 11
7b. The finite element discretization for section x = 99.06m 12
7c. The finite element discretization for section x = 0.00m 13
8a. Major principal stress contours, under loading A, for section x = 102.87m . . 17
8b. Minor principal stress contours, under loading A, for section x = 102.87m . . 18
9a. Major principal stress contours, under loading A, for section x = 95.25m . . 19
9b. Minor principal stress contours, under loading A, for section x = 95.25m . . 20
10a. Major principal stress contours, under loading A, for section x = 88.39m . . 21
10b. Minor principal stress contours, under loading A, for section x = 88.39m . . 22
11a. Local factor of safety in terms of Drucker/Prager yield function, ... (C=1 MPa, $\phi = 40°$), under loading A, for section x = 102.87m 23
11b. Local factor of safety in terms of Drucker/Prager yield function . . . . . (C=2 MPa, $\phi = 40°$), under loading A, for section x = 102.87m 24
12a. Local factor of safety in terms of Drucker/Prager yield function . . . . . (C=1 MPa, $\phi = 40°$), under loading A, for section x = 95.25m 25
11b. Local factor of safety in terms of Drucker/Prager yield function . . . . . (C=2 MPa, $\phi = 40°$), under loading A, for section x = 95.25m 26
13a. Local factor of safety in terms of Drucker/Prager yield function . . . . . (C=1 MPa, $\phi = 40°$), under loading A, for section x = 88.39m 27
13b. Local factor of safety in terms of Drucker/Prager yield function . . . . . (C=2 MPa, $\phi = 40°$), under loading A, for section x = 88.39m 28
14a. In-plane displacements for section x = 106.68m 30
14b. Out-of-plane displacements for section x = 106.68m 31

1.0 INTRODUCTION

A co-operative reseach project was initiated in 1985 with the active participation of the Niobec Mine Ltd., Centre de Recherches Minérales, Quebec, and Mining Research Laboratories, CANMET. The objectives of this project were:

(a) to contribute to the development of a geomechanical data-base on the physical and mechanical properties of mine rocks;

(b) to determine in-situ stresses at the mine site, and to design and install instruments for monitoring stress changes as mining progresses;

(c) to assess regional and local stability;

(d) to provide guidelines for mine design and ground control.

Numerical modelling is an integral part of this project. A series of three dimensional (3-D) finite element simulations will be carried out for the purpose of mine stability assessment. The subject of this report, is a preliminary stability assessment of C-103-23 stope under gravitational loading.

2.0 THE NIOBEC MINE

2.1 Geological Background

The Niobec Mine is situated in a portion of the St. Honoré Carbonatite Complex (650 m.y. old) some 13 Km (8 miles) north-east of Chicoutimi, Quebec.

The St. Honoré Carbonatite Complex, one of several regional intrusives, is located in the Pre-Cambrian Grenville Province of the Canadian Shield. The carbonatite and satellite rocks are covered by a capping of Paleozoic (584 m.y. old) limestone [1].

This sedimentary rock belongs to the Trenton group of Ordovician period. More specifically, to the Tétrauville formation.

Carbonatite is a rock formed from rich carbonate mineral derivatives after a differentiation process from oceanic type subcrustal olivine basaltic magma.

The St Honoré carbonatite, as shown in Fig. 1, is approximately 3.2 km in diameter in a kidney shape with well differentiated lithologic units:

a) The central core consists of unit C_1 and C_2 which are coarse-grained dolomitic carbonatites. C_1 is rich in rare earths and niobium but with chloritic and hematitic alteration. C_2 is sterile in rare earths and unaltered.

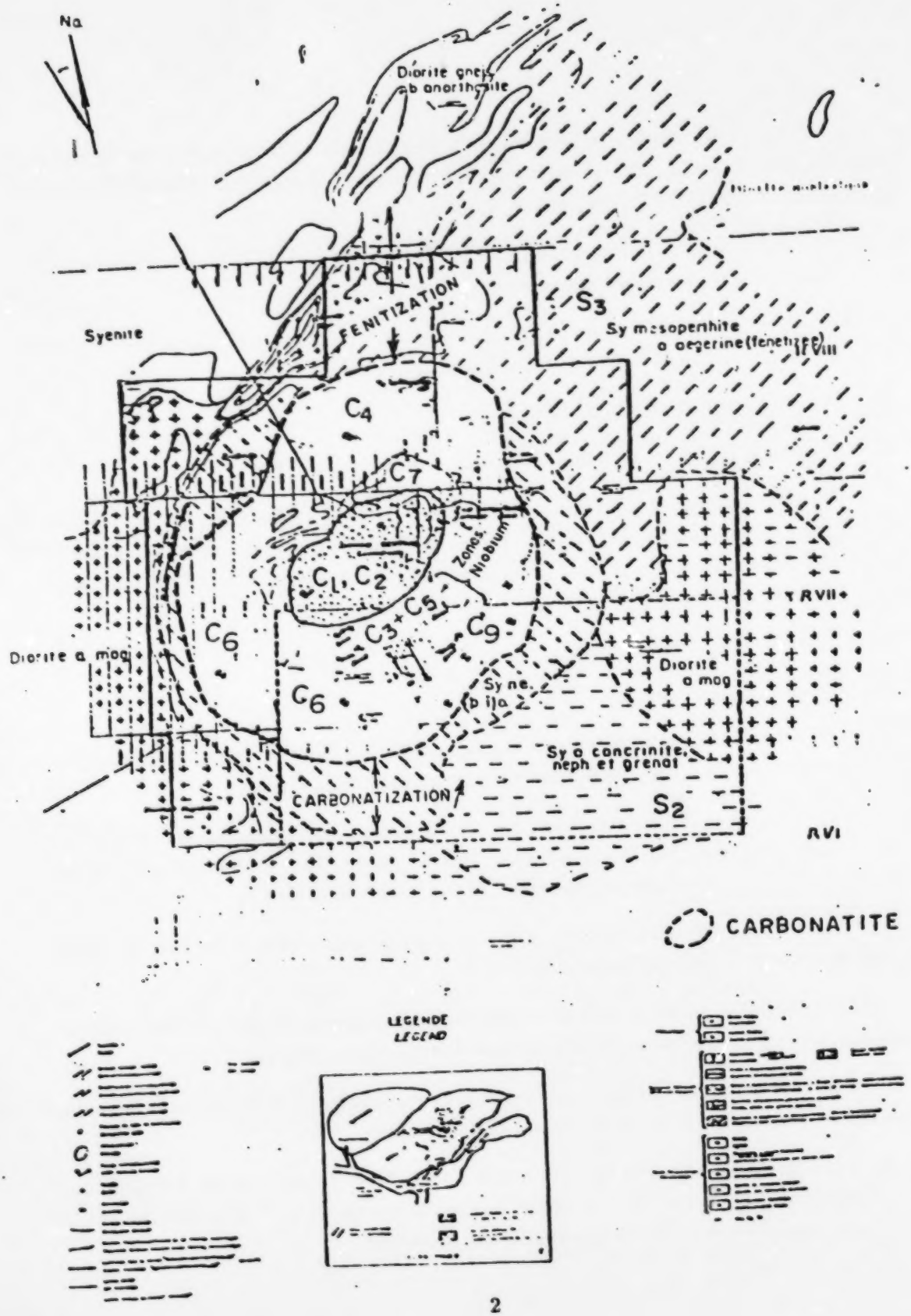

Fig. 1 Regional geology of Niobec Mine

b) The outer ring consists of dolomitic carbonatite (C_3, C_5, C_7, C_9) or magnetitic/calcitic carbonatite (C_4, C_6). Their features are:

C_3 - foliated to brecciated, fine to medium-grained; niobium occurs in high concentration.

C_4 - foliated, fine- grained; low niobium concentration.

C_5 - massive, fine to medium-grained; some banded alterations; low niobium concentration.

C_6 - foliated to massive, medium to coarse-grained; low niobium concentration.

C_7 - foliated, medium-grained; no niobium concentration.

C_9 - massive, fine-grained with strong hematitic alteration; no niobium concentration.

The structural discontinuities developed in the deposit can be classified into two categories: (a) large, sub-horizontal (85%), and some vertical (15%), extension joints created by the cooling of intrusive; and (b) small joints with predominantly horizontal and subvertical orientation. The latter, usually less than 50 cm, occurs throughout the mass in a discontinuous non-intersecting fashion. The sub-horizontal joints predominate at greater depth, the sub-vertical ones occur occasionally throughout the mine; their intersection creating '$\top$' or '$\perp$' patterns.

No major faulting has been revealed. As well, no significant ground water seepage has been observed.

2.2 General Mining Conditions

A typical longitudinal view of the Niobec Mine is shown in Fig. 2. Figure 3 shows a typical open stope layout.

The mining pattern at the Niobec Mine follows the economical concentration of niobium outlined in the interconnected vertical pods. The numerous concentrations are irregularly distributed in the main carbonatite body, therefore, an irregular open stoping method is employed.

Two tiers of operations presently exist at the mine. The upper tier is from the overlying limestone-intrusive contact (level 250 to 300) to level 600. The second tier, separated from the first tier by a 33m (100 ft) sill pillar, has stopes developed to level 1000. Stopes in the lower tier follow the same pattern as stopes in the upper tier with some lateral shift

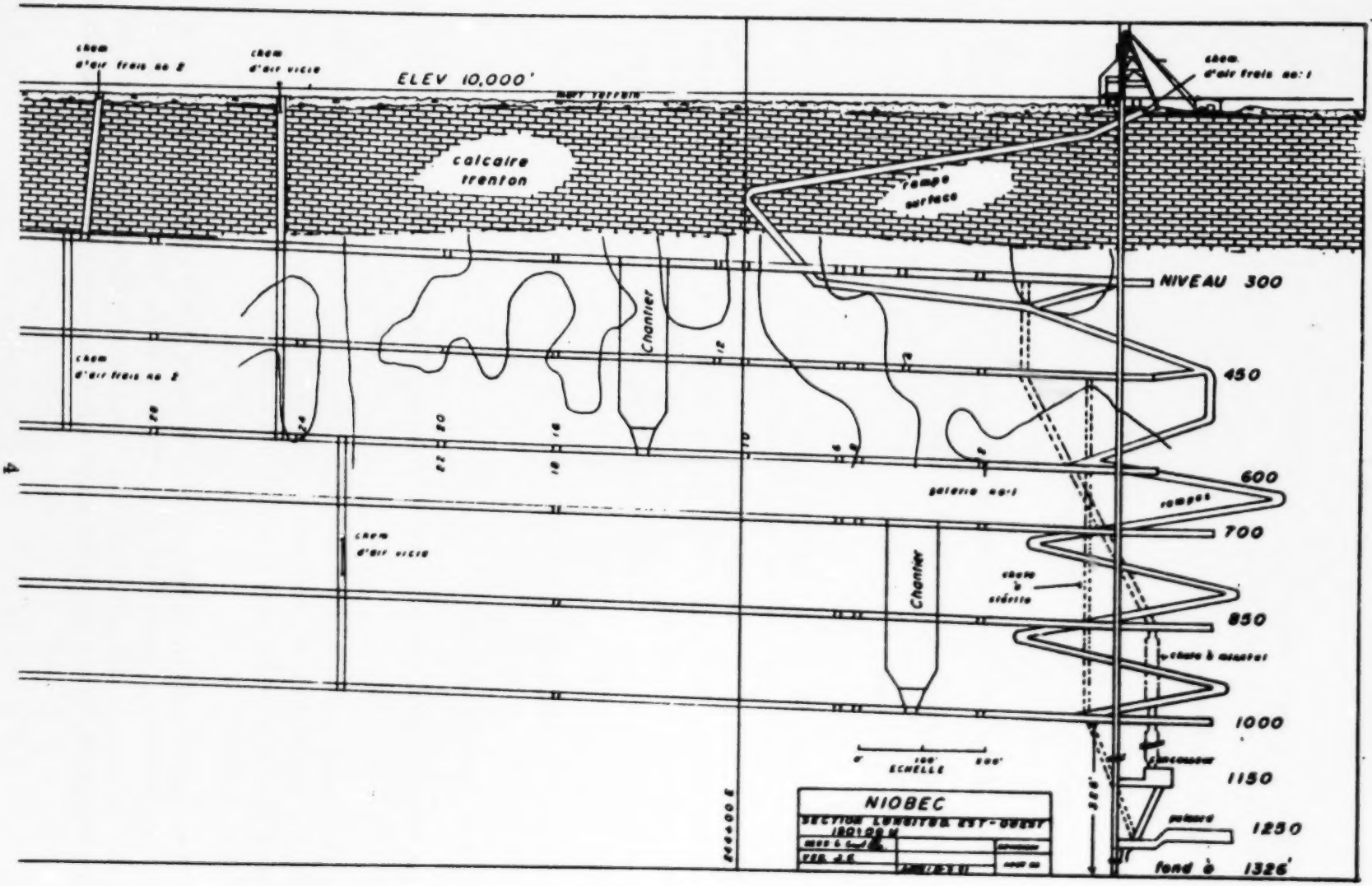

Fig. 2 A typical cross sectional view of the Niobec Mine

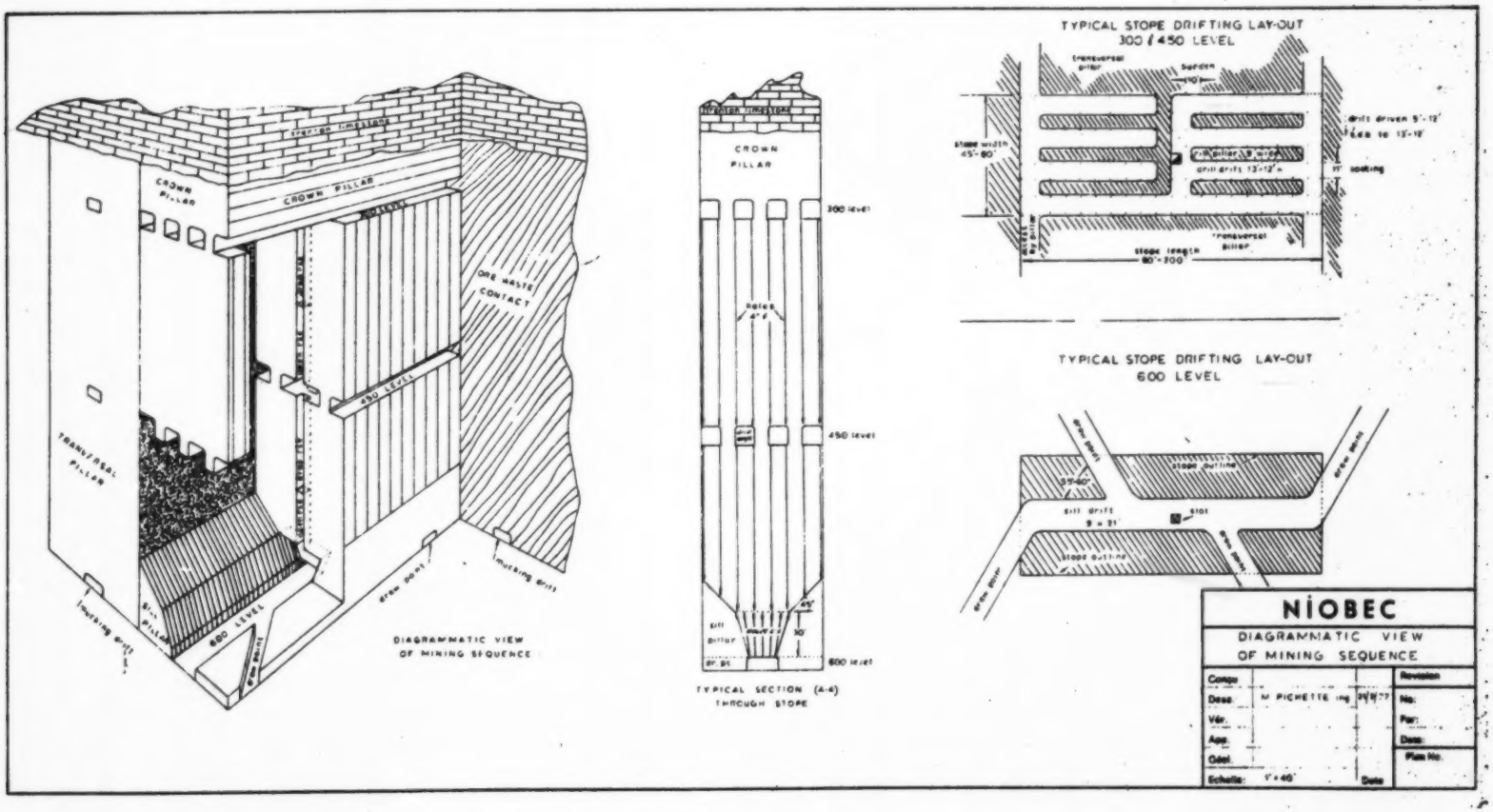

Fig. 3 A typical open stope layout

due to the mineralization dip.

For economic reasons, no backfill has been used at the Niobec Mine. As a result, stopes with a minimum height of 100 metres have been left open since excavation. The roofs of these stopes have been strengthened through the use of mechanical bolts, but the stope walls (primarily pillars) are unsupported. Sloughing never exceeds 3-4% of the original volume mined.

The drifts, 3m x 4m in dimensions, are excavated using pre-split blasting. Drift walls are unsupported, but the backs are supported when required. In the worst areas both bolting and screening are used.

Except for Zone 1, primary stoping in the upper tier has been completed. Secondary stoping of economical pillars is planned. In the lower tier, limited primary stoping has been taken place primarily in the area of the shaft.

At present, the mine has no major ground control and stress problems because it is currently operating at shallow depth (no deeper than 300m) and the rock mass is generally competent with only intermittent discontinuities.

However, several forms of local instability have occurred.

a) Between the 700 and 900 levels numerous, extensive, altered sub-horizontal joints are present. This has resulting joint opening, roof separation and block formation.

b) Unpredictably, weak rock pockets have been located throughout the intrusive that have produced falls of 100 to 50,000 m^3 of rock. Weak rock pockets consist of small-sized biotite covered fragments which have never been stable when exposed in an opening.

c) As the carbonatite transition zone forms the bottom of a surface crown pillar and exceeds 2m in thickness, it is usually stable; however, when the thickness is less than 2m, it detaches itself from the limestone.

2.3 Mine Layout

Figure 4 is a plan view of level 300. Figure 5 shows longitudinal section (157 + 50N). Stopes C-102-21, C-102-19, C-102-17 and C-102-15 have been completely mined leaving pillars L-102-17 and L-102-15 intact. Standard mine layout in this mine calls for 24m (80 ft) wide stopes separated by 24m wide pillars. The ground in the upper tier of Niobec Mine is considered competent. Development work is presently being carried out in the area of proposed stope C-102-23, as shown in Figs. 3 and 4. It is planned to mine

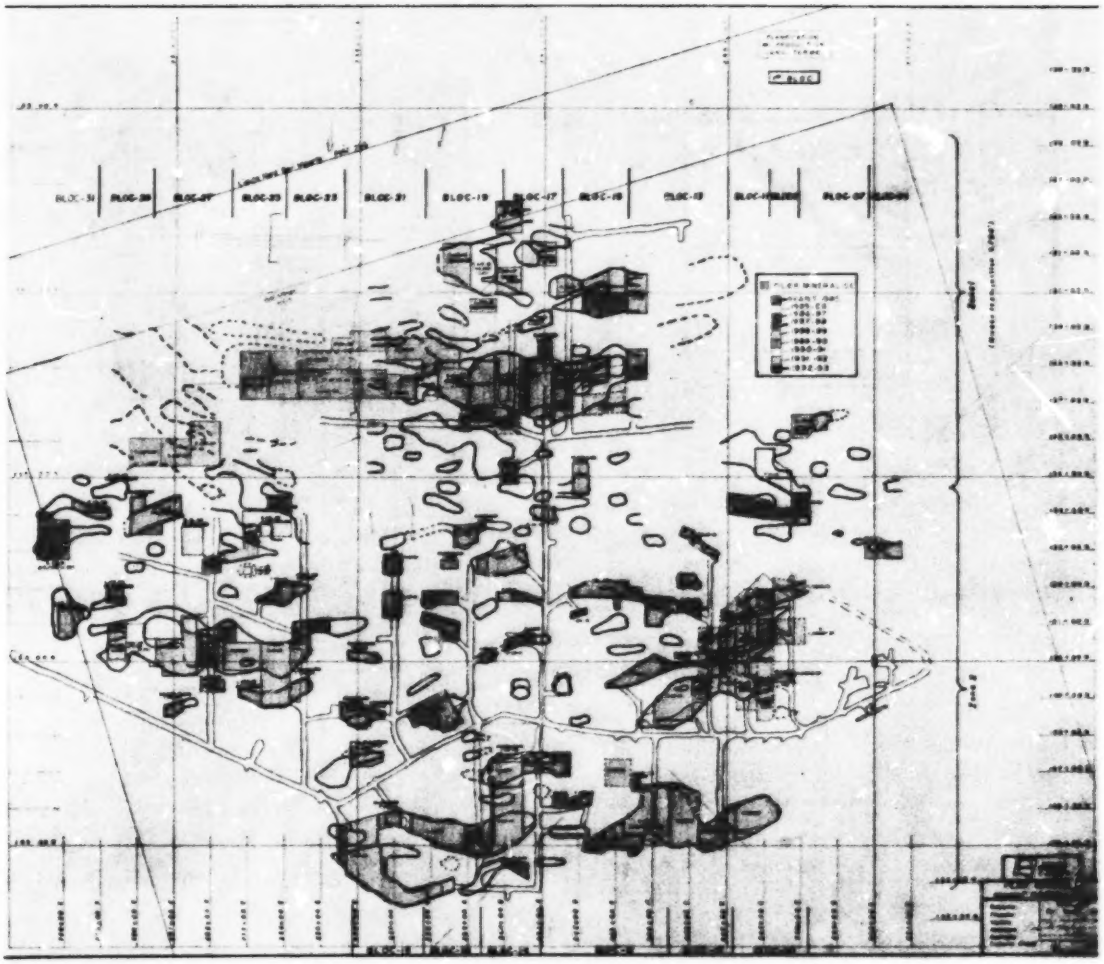

Fig. 4 Plan view of the Mine at level 300

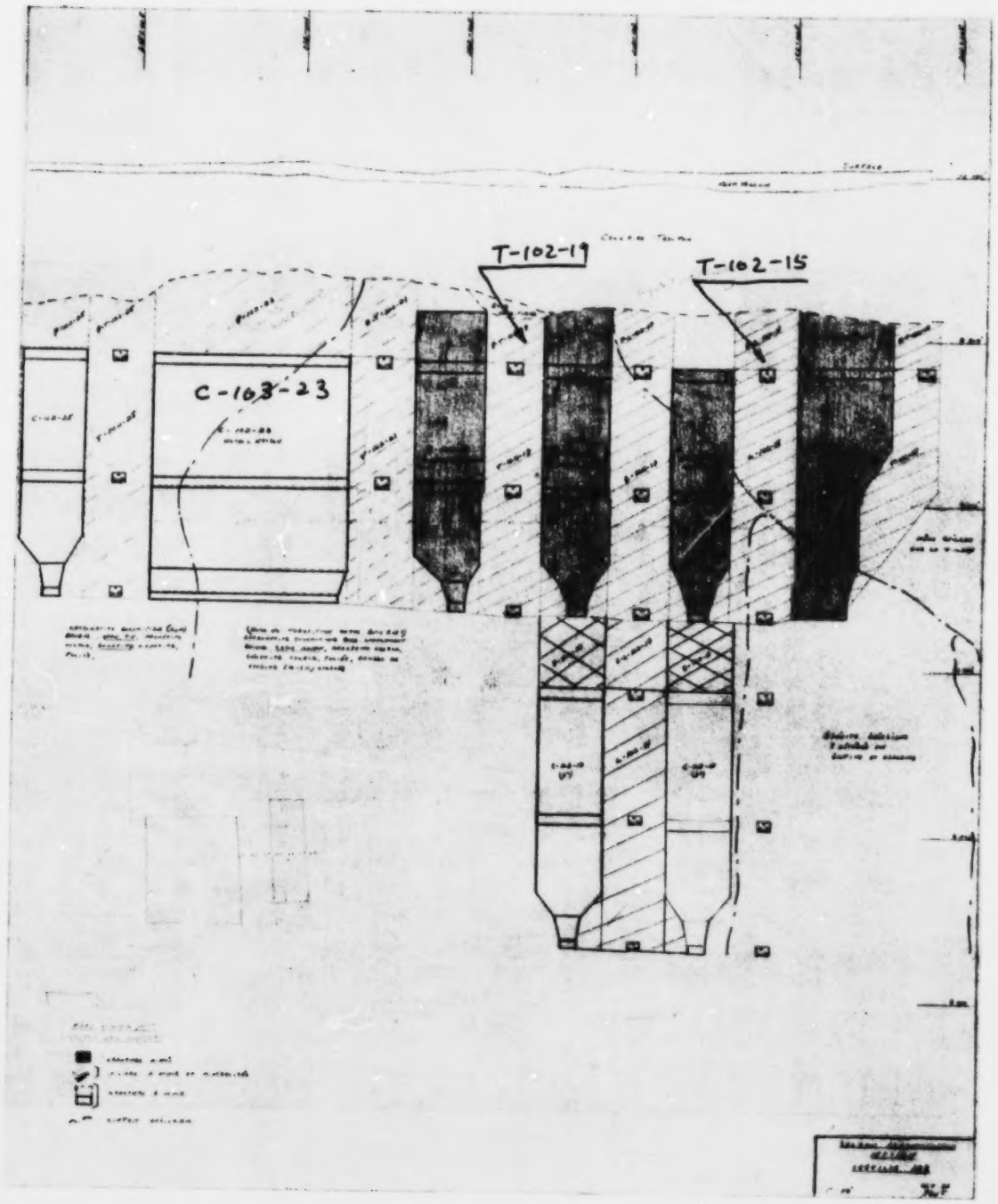

Fig. 5 Longitudial section 157 + 50N

C-102-23 in 1987 as one large stope; the stope span will be approximately 73m (240 ft). The mine is concerned about the stability of this stope and adjacent stopes and pillars because of the large stope span.

2.4 3-D Niobec Mine model

To assess the structural stability of proposed C-102-23 stope and adjacent mine structures, a three-dimensional finite-element model was constructed for analysis purposes.

Since the mine structure is essentially infinite, it is necessary to truncate the structure so that it can be modelled economically. A choice has to be made between a large, accurate model with high computer costs and a smaller, less accurate model with lower costs.

The 3-D model constructed for this study has the following dimensions: 635m long (along the 157 + 50N longitudinal section), 213m thick, and 330m high. The model consists of two wide stopes 73.15m (240 ft) wide, 91.44m (300 ft) high and 24.38m (80 ft) thick; and two narrow stopes 24.38m wide, 97.53m high and 24.38m thick. All stopes are separated by 24.38m (80 ft) wide pillars.

Figure 6 is an isometric view of the mine model. To simplify mine geometry for modelling purpose, T-102-19 pillar and stope C-103-23 have been assumed to be symmetric around central planes, therefore, only one quarter of the structure had to be simulated. However, it should be noted that the larger stope on the right hand side of the plane of symmetry (mirror image of stope C-103-23, not shown in Fig. 6) is actually two small stopes separated by a 24.38m wide pillar. For simplicity and economy in computing costs, pillar L-102-15 was considered mined-out. Thus it became part of the large stope (combining with stopes C-102-17 and C-102-15). The approximations in terms of the actual mine geometry should provide a conservative estimate of its state in terms of stresses or failure conditions.

The model as shown in Fig. 6, is divided into eight slices (nine sections) with thickness varying from 7.62m (25 ft) to 34.48m (113 ft). Three typical cross sections with their finite element discretizations are shown in Fig. 7(a) to Fig. 7(c). Two adjacent plane sections forms one three-dimensional slice which yields 418 eight-node brick elements and 920 nodes. Thus, the model has a total of 3344 elements and 4140 nodes.

2.5 Computer Program

The three-dimensional (3-D) finite element formulation is based on certain assumptions concerning the displacements field and the principle of minimum potential energy. The theory on which it is based and the derivation of formulation have been described in detail elsewhere [2,3].

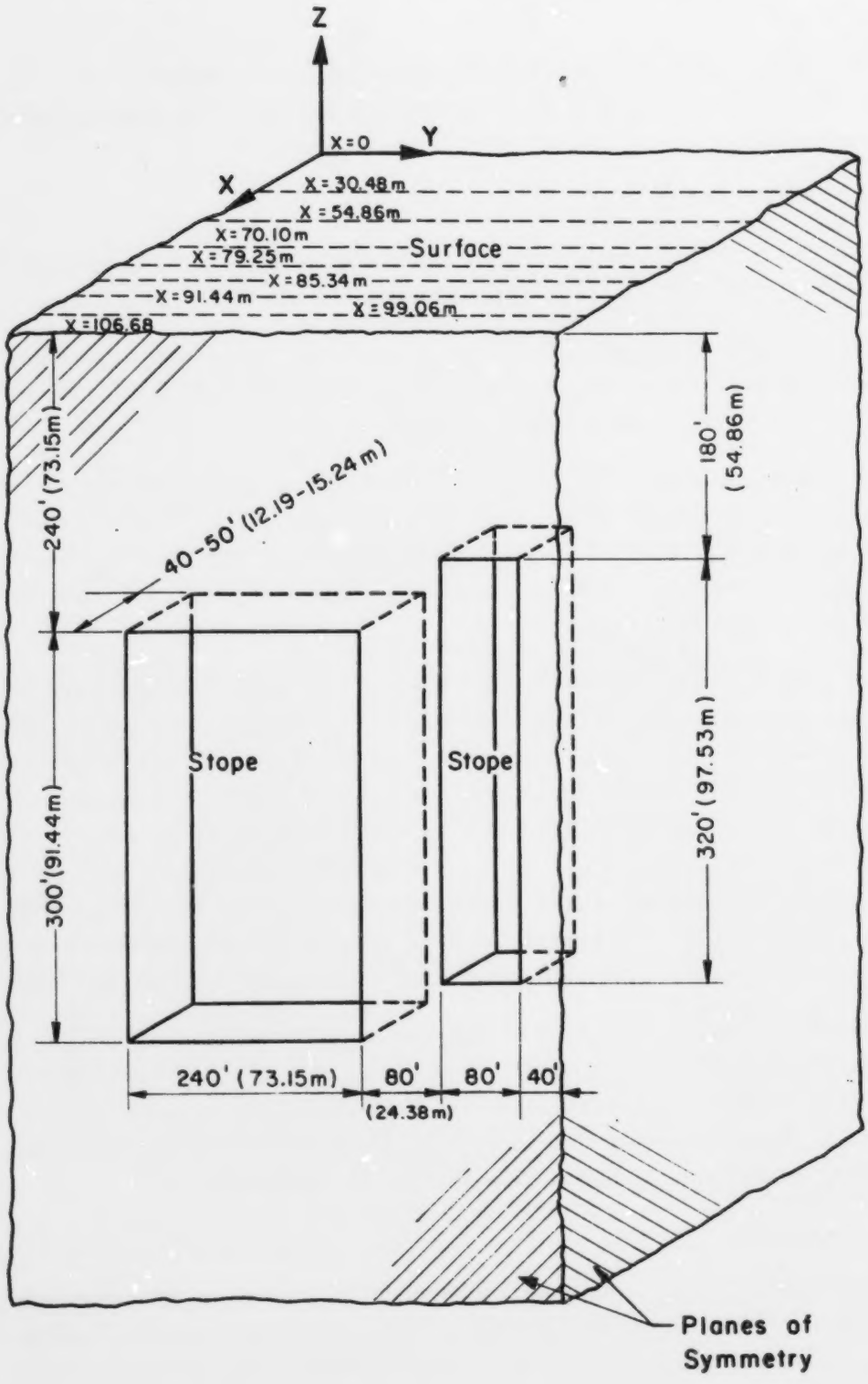

Fig. 6 Isometric view of the Mine Model

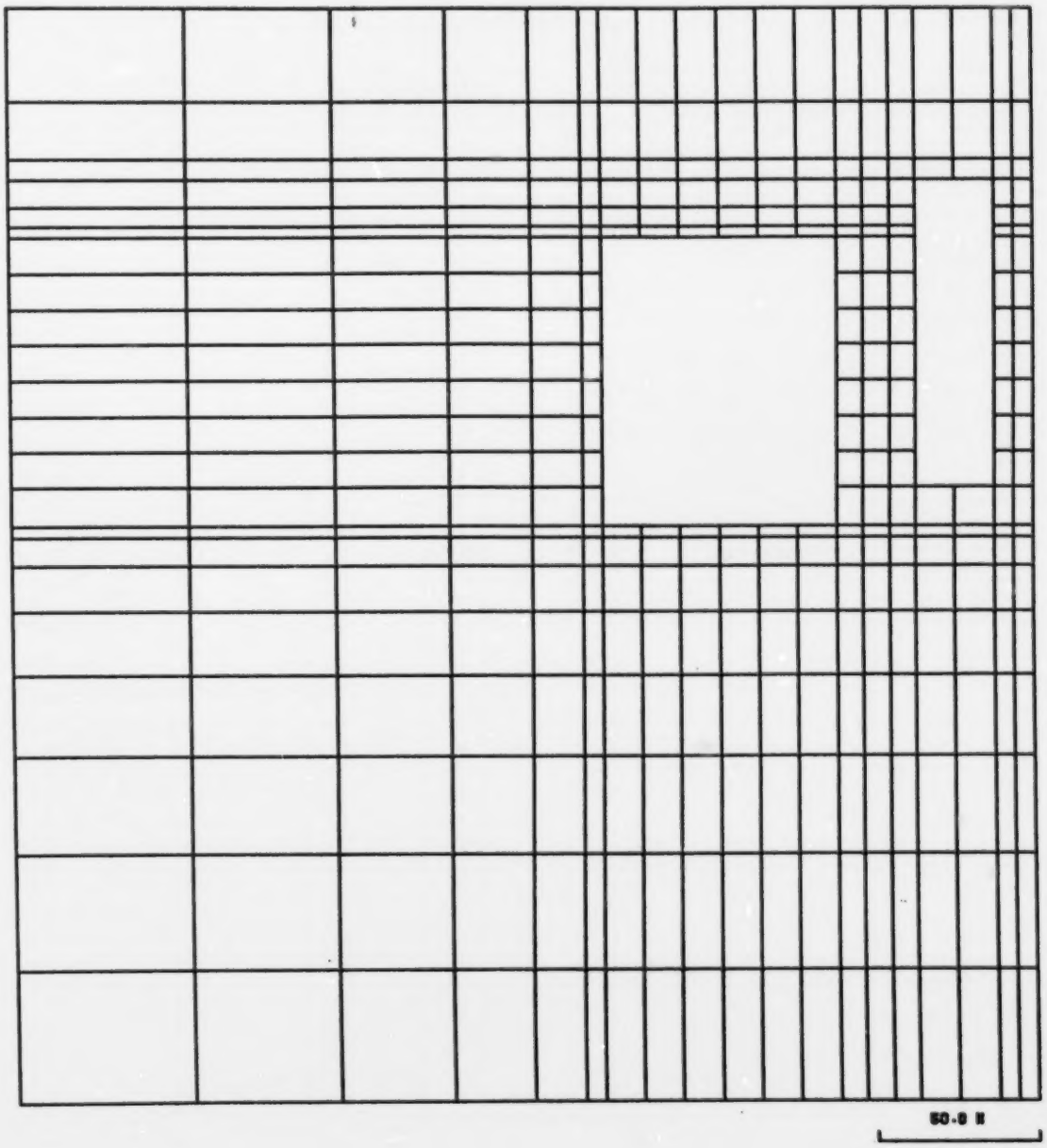

Fig. 7(a) The Finite Element Discretization for Section x=106.68 m.

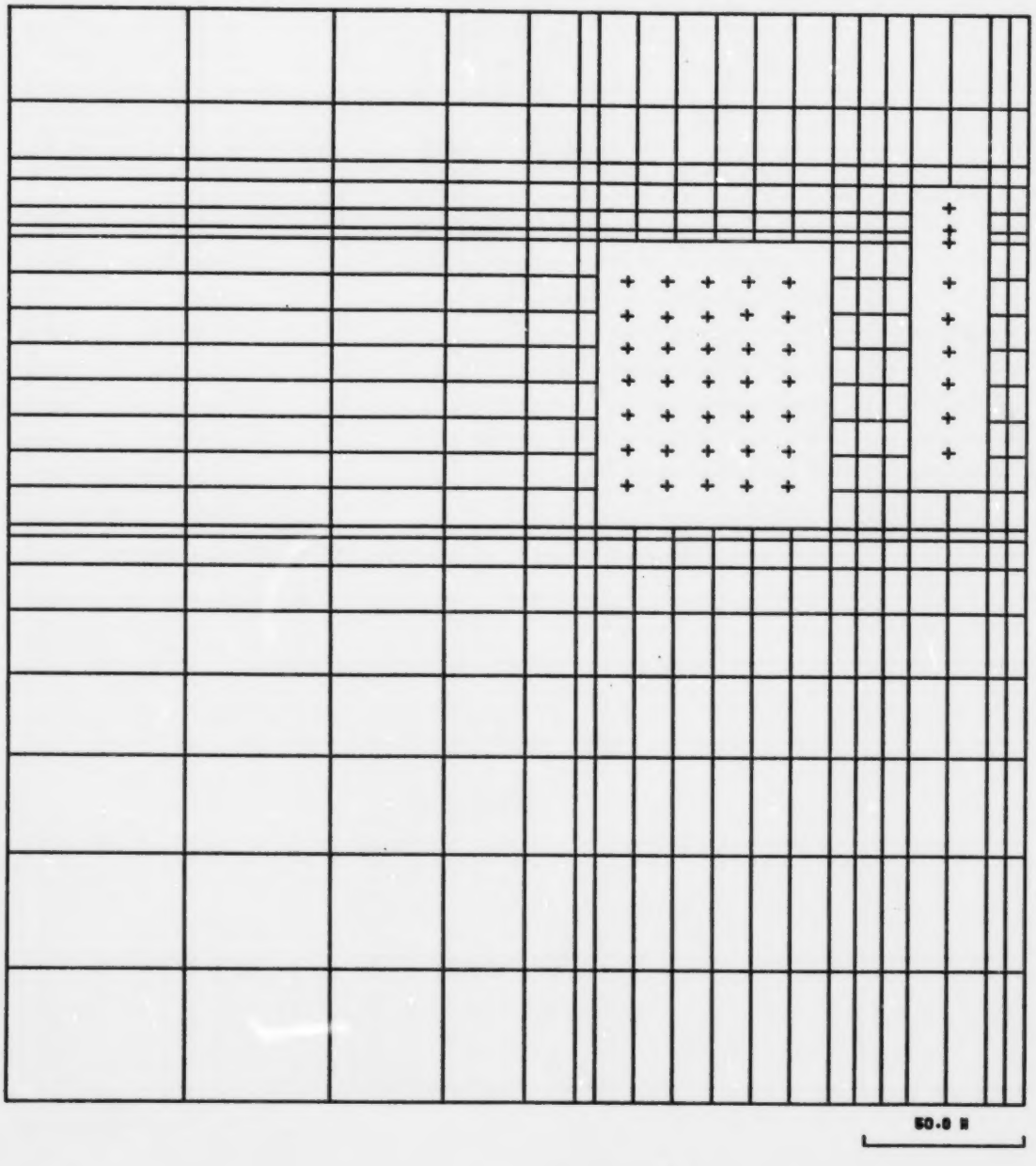

Fig. 7(b) The Finite Element Discretization for Section x=99.06 m.

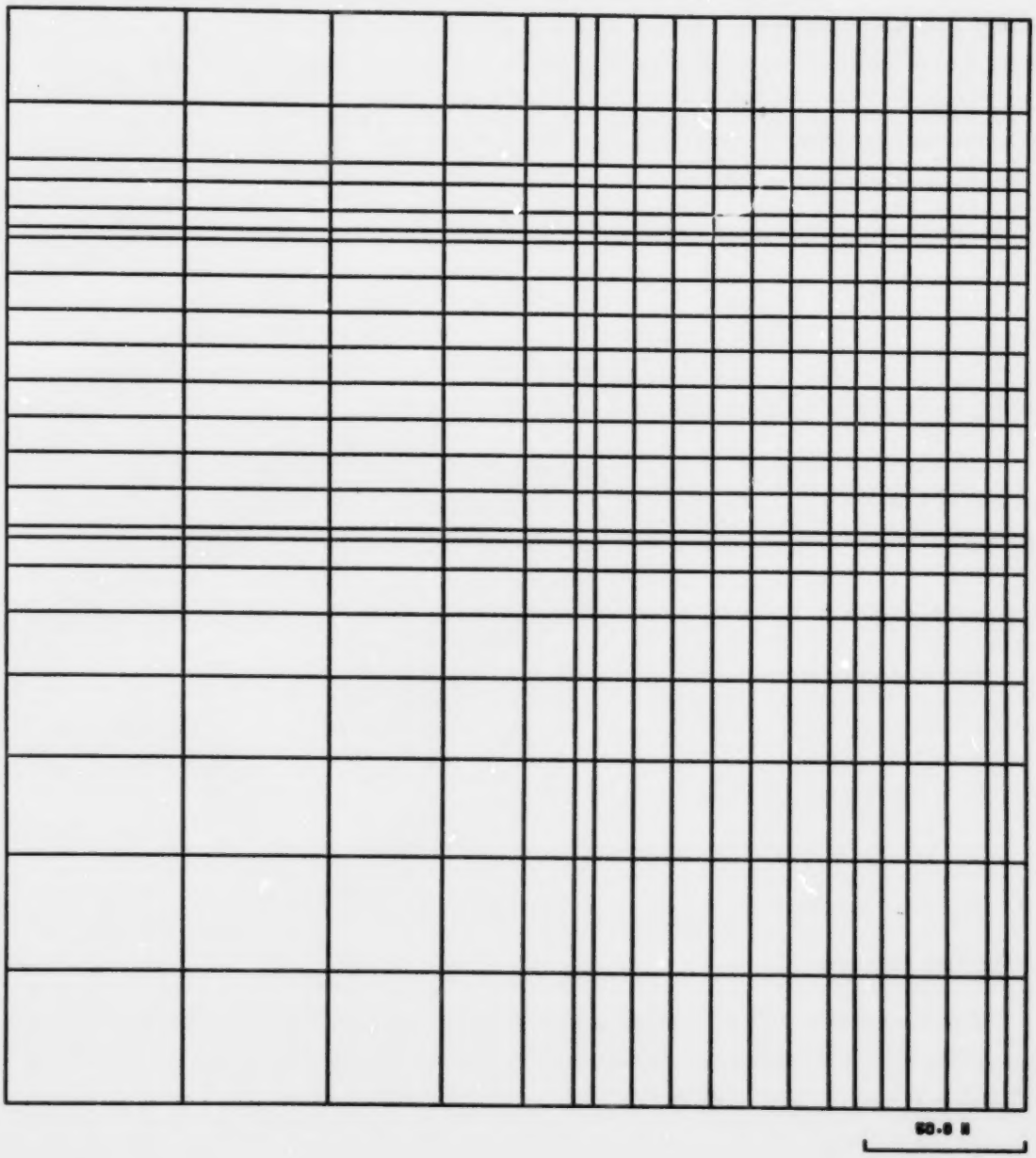

Fig. 7(c) The Finite Element Discretization for Section x=0.0 m.

The computer program used for this study was originally developed by Prof. E.L. Wilson of the University of California [2] and has been extensively modified at the Mining Research Laboratories to meet our requirements, to improve efficiency and to reduce costs.

The basic eight-node brick element with three degrees of freedom at each node, which assumes a tri-linear displacement field, is used in the program for three-dimensional analysis. The program performs static, and linear elastic analysis. Material properties are assumed to be isotropic. The program is capable of handling gravity and distributed surface loads. Initial residual stresses, if known, can also be used as input. Mesh generation for certain geometries is also incorporated [4].

2.6 Material Properties of Mine Rocks

Testing the mechanical properties of various mine rocks was carried out by Centre de Recherches Minérales, Quebec. Since such information was not available when the the 3-D Niobec model was constructed and preliminary analysis carried out. Input rock parameters selected on the basis of experience were used.

Because mining is taking place in a massive carbonatite formation, variation of the physical and mechanical properties from the hangingwall to footwall is considered minimal. The massive carbonatite is covered by approximately 60m (200 ft) of massive limestone. The latter is also assumed to have limited variation with locations in its physical and mechanical properties. Both formations in the model are treated as linear elastic materials.

The following are the rock input parameters used in the model:

Carbonatite: $E = 40\ GPa,\ \ \nu = 0.25$

Limestone : $E = 30\ GPa,\ \ \nu = 0.25$

where: E = Modulus of elasticity, and ν = Poisson's ratio.

The unit weight of both rocks, γ, is assumed to be 0.027 MN/m^3.

2.7 In-Situ Stresses

The magnitudes of pre mining stresses were not available at the time the analysis was conducted. To establish pre mining stresses for the model, gravitational loading was used and is referred to as Loading A.

Loading A: $\sigma_z = \gamma Z$

$$\sigma_x = \sigma_y = \frac{\nu}{(1-\nu)}$$

where σ_z is the vertical stress at depth Z; σ_x and σ_y are the horizontal stresses; γ is the unit weight of the rock material; ν is Poisson's ratio.

3.0 RESULTS

The output of a three-dimensional finite element analysis provides a large amount of information. The analysis and interpretation of results would be extremely tedious if done manually. Thus programs have been developed to represent graphically the displacements and stresses in a vector and/or point contour form.

Three-dimensional vectorial representation for stresses and displacements would be very confusing to the reader because of the massive data to be displayed in a relatively small area. Consequently, in this report, the principal stresses (major and minor) are presented in a contour form for different 'slices' of the mine model; intermediate principal stresses are not plotted. The displacements were separated into in-plane and out-of-plane vectors. For an in-plane vector the resultant of the y - and z - components of the displacements were plotted with an appropriate direction and scale; the out-of-plane vector directed either in increasing x - direction or decreasing x - direction were plotted separately. Usually the out-of-plane displacements are small when compared with in-plane vectors.

Frequently, there is an interest in defining a local factor of safety. This is some scalar function of stresses that is assumed to determine stability. In this study, a normalized Drucker/Prager yield function was selected. (see Appendix A).

In this study, two sets of material constants were used to calculate local factors of safety, namely:

Case 1: $C = 1\ MPa$, and $\phi = 40°$.

Case 2: $C = 2\ MPa$, and $\phi = 40°$.

where: C is the cohesion, and ϕ is the angle of internal friction.

Note that the sign convention of stresses presented below are compressive stress positive, and tensile stress negative.

3.1 Stress Distribution

Figures 8, 9, and 10, show the principal stress contours around C 102-23 stope at sections x = 102.87m, 95.25m, and 88.39m, respectively. Stresses for section x = 102.87m, represent the average stresses at the central portion of the stope. Section x = 88.39m is

located at about 3m (10 ft) in from the hangingwall or footwall. All stresses are calculated at the centroid of each element, which is located at the middle plane of each 'slice'.

The contour plots indicate that the mining of C-102-23 stope does not create large magnitude compressive stresses around the stope; however, tensile stresses are developed in the floor, roof and walls of stopes, and in pillar walls. Although the magnitude of these tensions are small, say 0.25 - 1.0 MPa, they might cause some local instability, such as the spalling of pillar and stope walls and roof separations, if joints are favorably oriented in relation to the direction of the tensile stresses. As well, floor heaving is expected. At the quarter span of C102-23 stope back, both the major and minor principal stresses for the near surface rock are tensile. It implies that cracks may initiate at that location, and may propagate throughout the tensile stress zone of the stope back. With an unfavorable combination of these tensile stresses and discontinuity, caving is anticipated. The shaded areas shown in Figs. 8(a), 8(b), 9(b) and 10(b) indicate potential failure zones.

3.2 Safety Factor

The factor of safety, using the Drucker/Prager yield function, is calculated for sections x = 102.87m, 95.25m and 88.39m. These are illustrated in Fig. 11, 12 and 13. As described earlier, two sets of the material constants were used in the calculations, i.e., Case (a) $C = 1\ MPa$ and $\phi = 40°$, and Case (b) $C = 2\ MPa$ and $\phi = 40°$. No yield zones (factor of safety $\leq$ 1.0) occurred in either cases (a) or (b). The values of C which range from 1 MPa to 2 MPa, are considered to be low and conservative; therefore, shear failure in the roof or in the pillars is not likely under the assumed loading conditions. It should be pointed out that factors of safety in the tensile zone appear to be high. This is due to the fact that the shear stresses are small. This relaxed area will not fail in shear.

3.3 Displacements

The predicted elastic displacements at the central section of C102-23 stope is shown in Fig. 14(a). The largest displacement occurs at the floor and is about 0.6cm. The out-of-plane displacement, as shown in Fig. 14(b) is negligible because of the plane symmetry.

It should be noted that these displacements are the total elastic displacements. In order to obtain the 'excavation' displacements as a result of mining these stopes, two separate computer runs should be conducted. The 3-D model would be run first without the stopes being excavated and then with the stopes excavated. In this preliminary study, the first run was not carried out. However, the patterns of the excavation displacements should be similar to those shown in Fig. 14(a), but the roof is slightly less sagged.

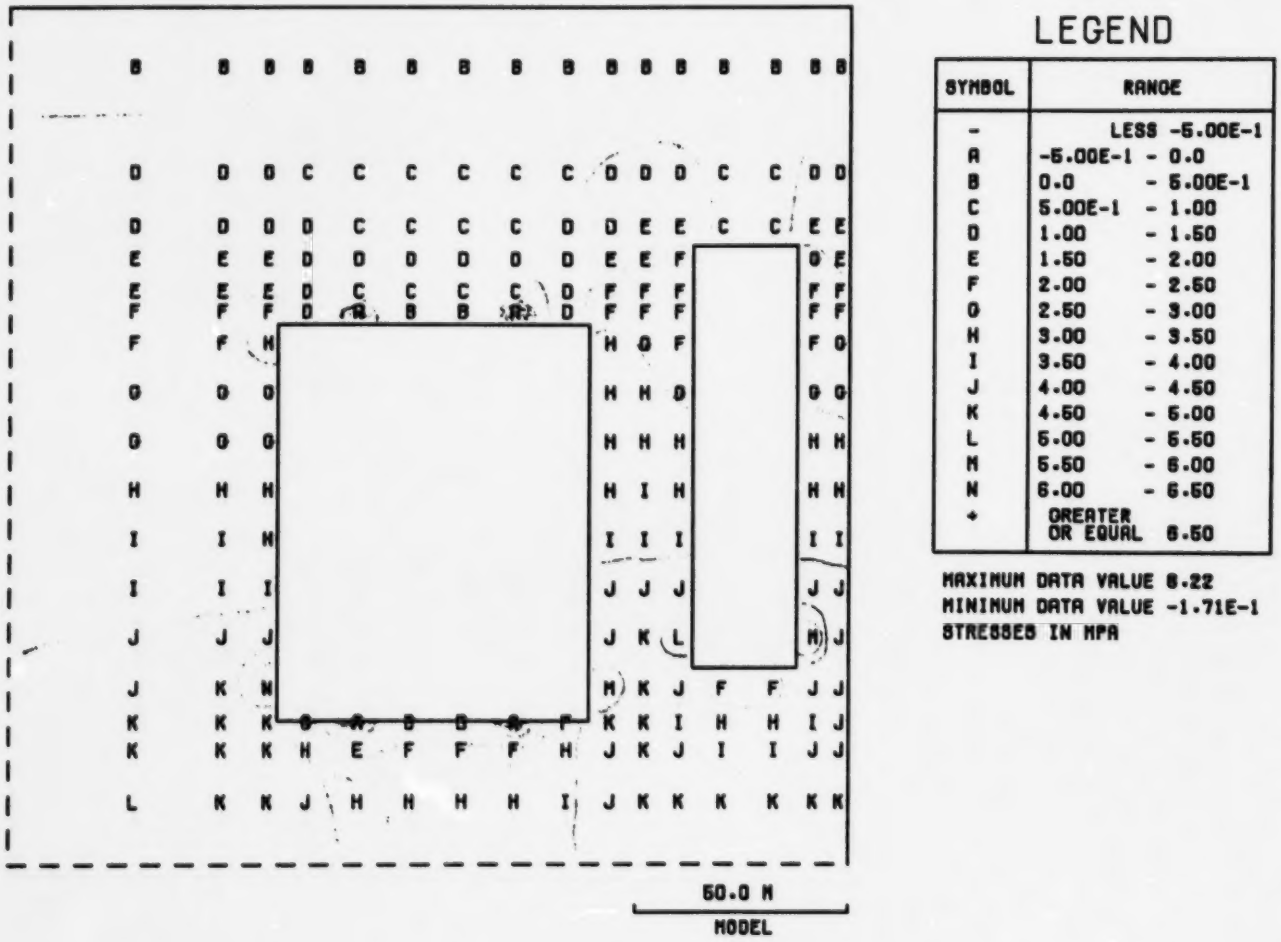

Fig. 8(a) Major Principal Stress Contour, Under Loading A, for Section x=102.87 m.

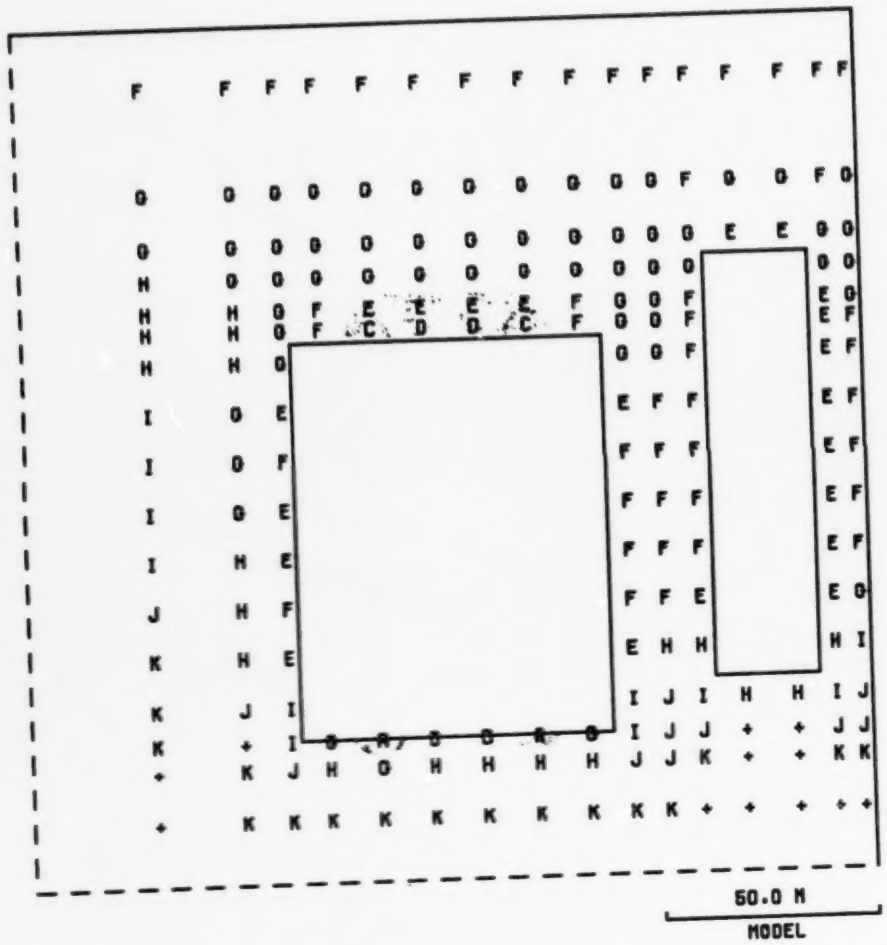

LEGEND

SYMBOL	RANGE
-	LESS -1.25
A	-1.25 - -1.00
B	-1.00 - -7.50E-1
C	-7.50E-1 - -5.00E-1
D	-5.00E-1 - -2.50E-1
E	-2.50E-1 - 0.0
F	0.0 - 2.50E-1
G	2.50E-1 - 5.00E-1
H	5.00E-1 - 7.50E-1
I	7.50E-1 - 1.00
J	1.00 - 1.25
K	1.25 - 1.50
+	GREATER OR EQUAL 1.50

MAXIMUM DATA VALUE 1.65
MINIMUM DATA VALUE -1.02
STRESSES IN MPA

Fig. 8(b) Minor Principal Stress Contour, Under Loading A, for Section x=102.87 m.

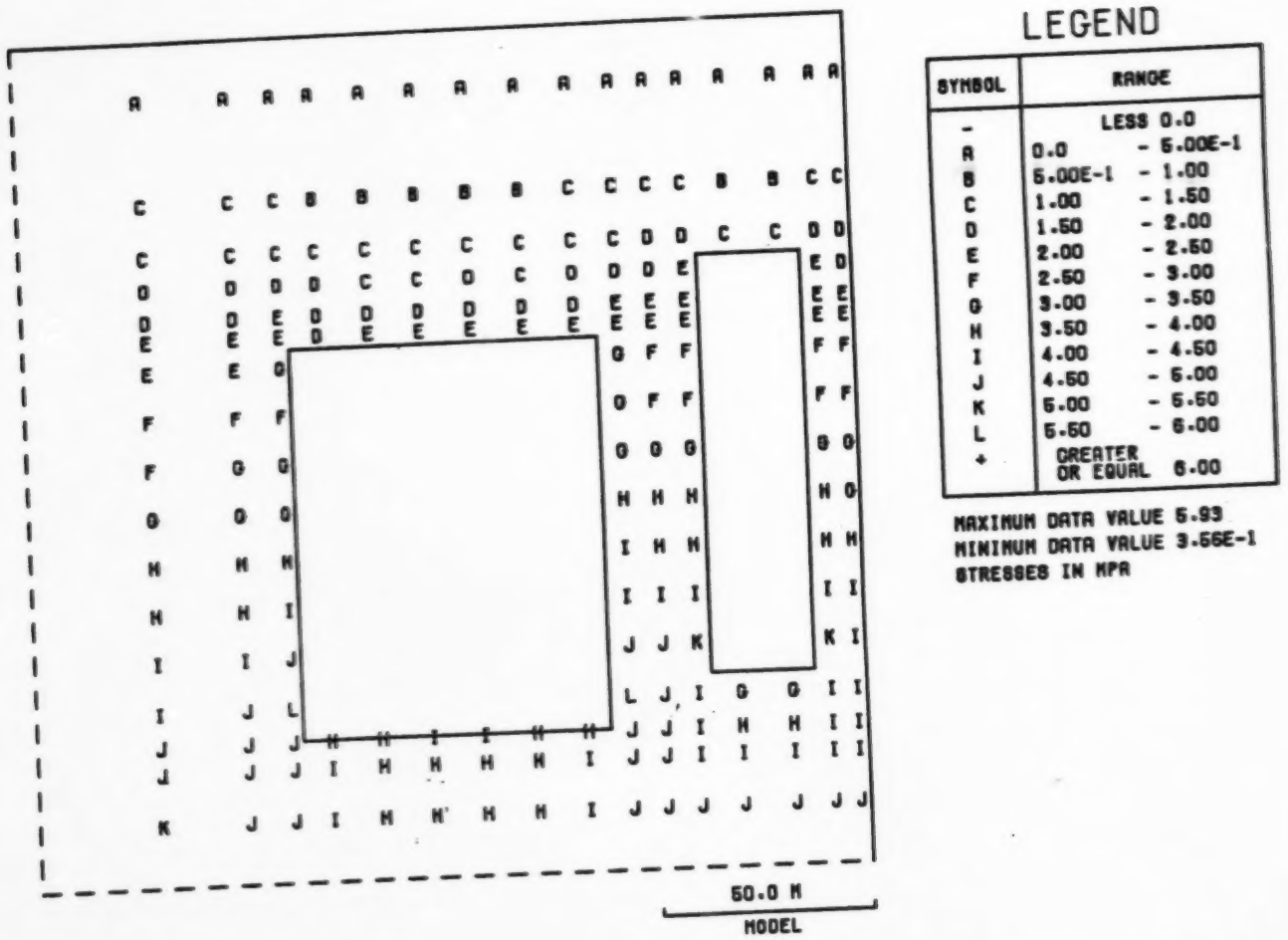

Fig. 9(a) Major Principal Stress Contour, Under Loading A, for Section x=95.25 m.

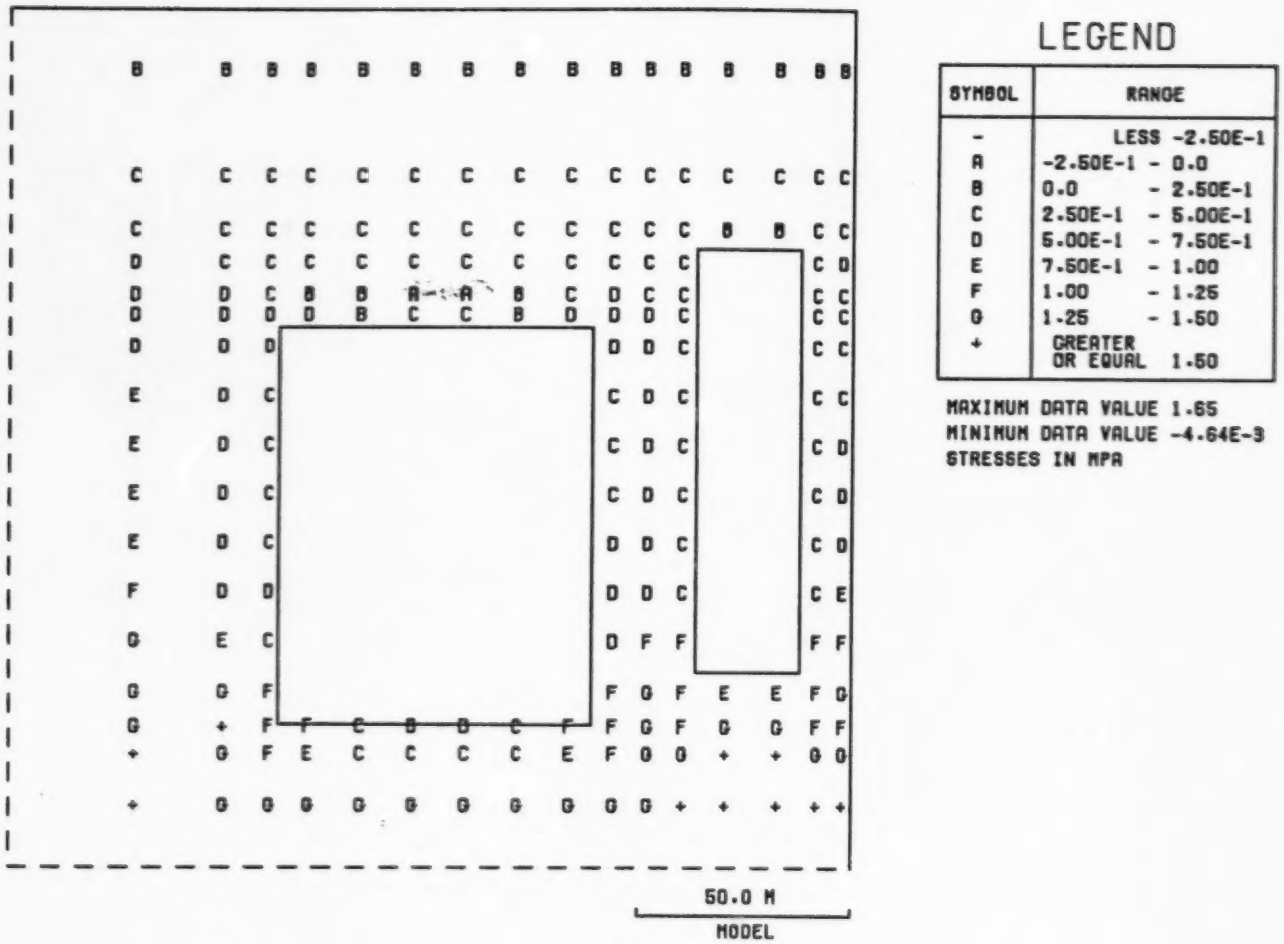

Fig. 9(b) Minor Principal Stress Contour, Under Loading A, for Section x=95.25 m.

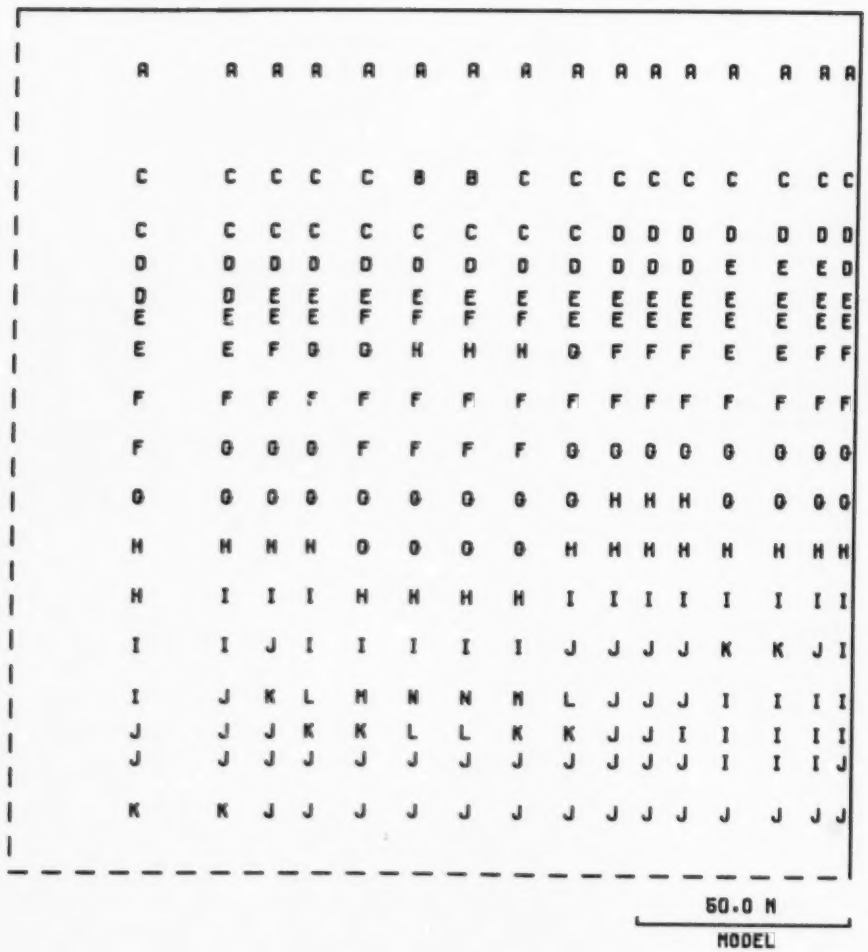

LEGEND

SYMBOL	RANGE
-	LESS 0.0
A	0.0 - 5.00E-1
B	5.00E-1 - 1.00
C	1.00 - 1.50
D	1.50 - 2.00
E	2.00 - 2.50
F	2.50 - 3.00
G	3.00 - 3.50
H	3.50 - 4.00
I	4.00 - 4.50
J	4.50 - 5.00
K	5.00 - 5.50
L	5.50 - 6.00
M	6.00 - 6.50
N	6.50 - 7.00
+	GREATER OR EQUAL 7.00

MAXIMUM DATA VALUE 6.57
MINIMUM DATA VALUE 3.78E-1
STRESSES IN MPA

Fig. 10(a) Major Principal Stress Contour, Under Loading A, for Section x=88.39 m.

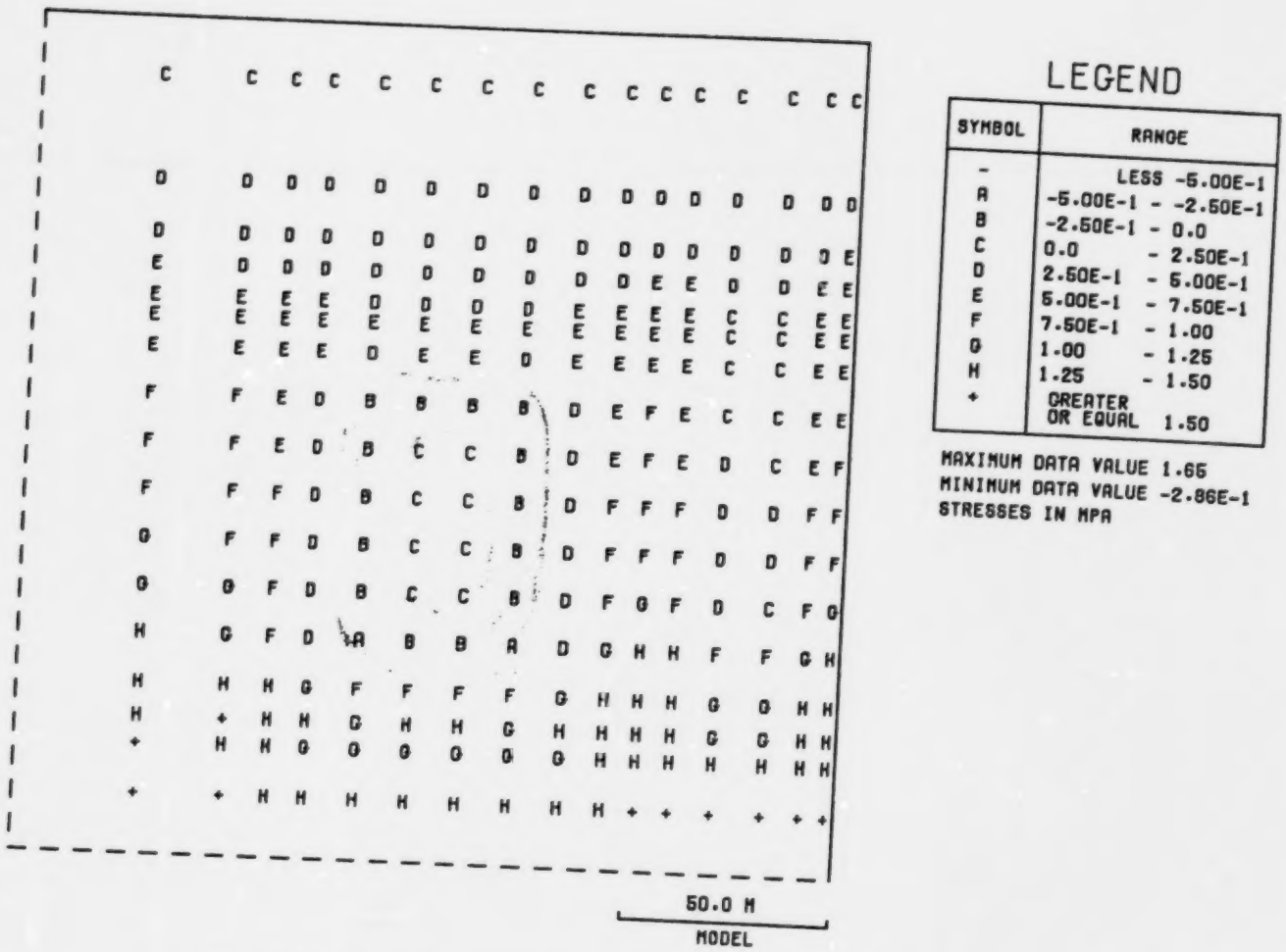

Fig. 10(b) Minor Principal Stress Contour, Under Loading A, for Section x=88.39 m.

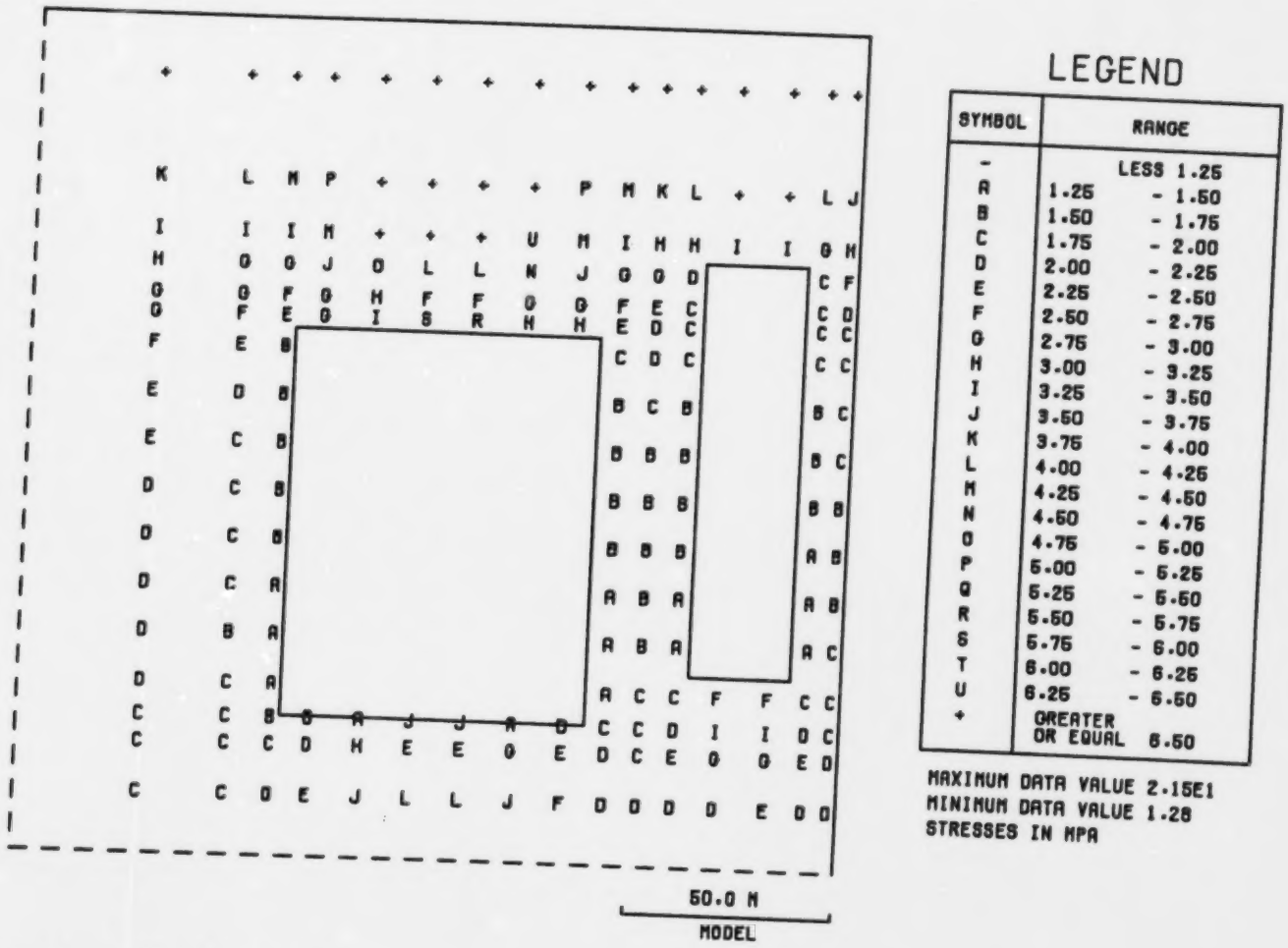

Fig. 11(a) Local Factor of Safety in Terms of Drucker/Prager Yield Function (C=1 MPa; $\phi = 40°$), Under Loading A, for Section x=102.87 m.

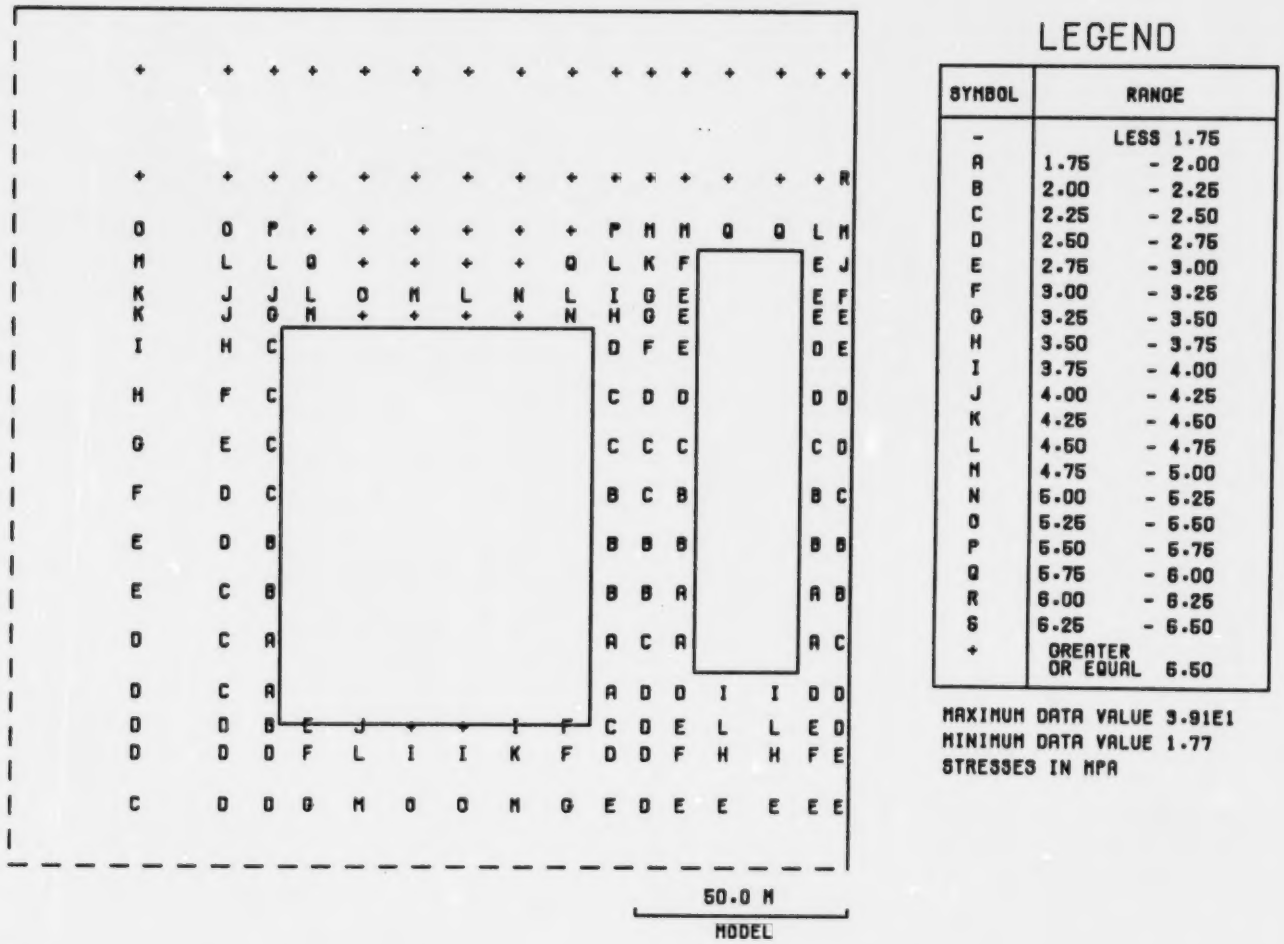

Fig. 11(b) Local Factor of Safety in Terms of Drucker/Prager Yield Function (C=2 MPa; $\phi = 40°$), Under Loading A, for Section x=102.87 m.

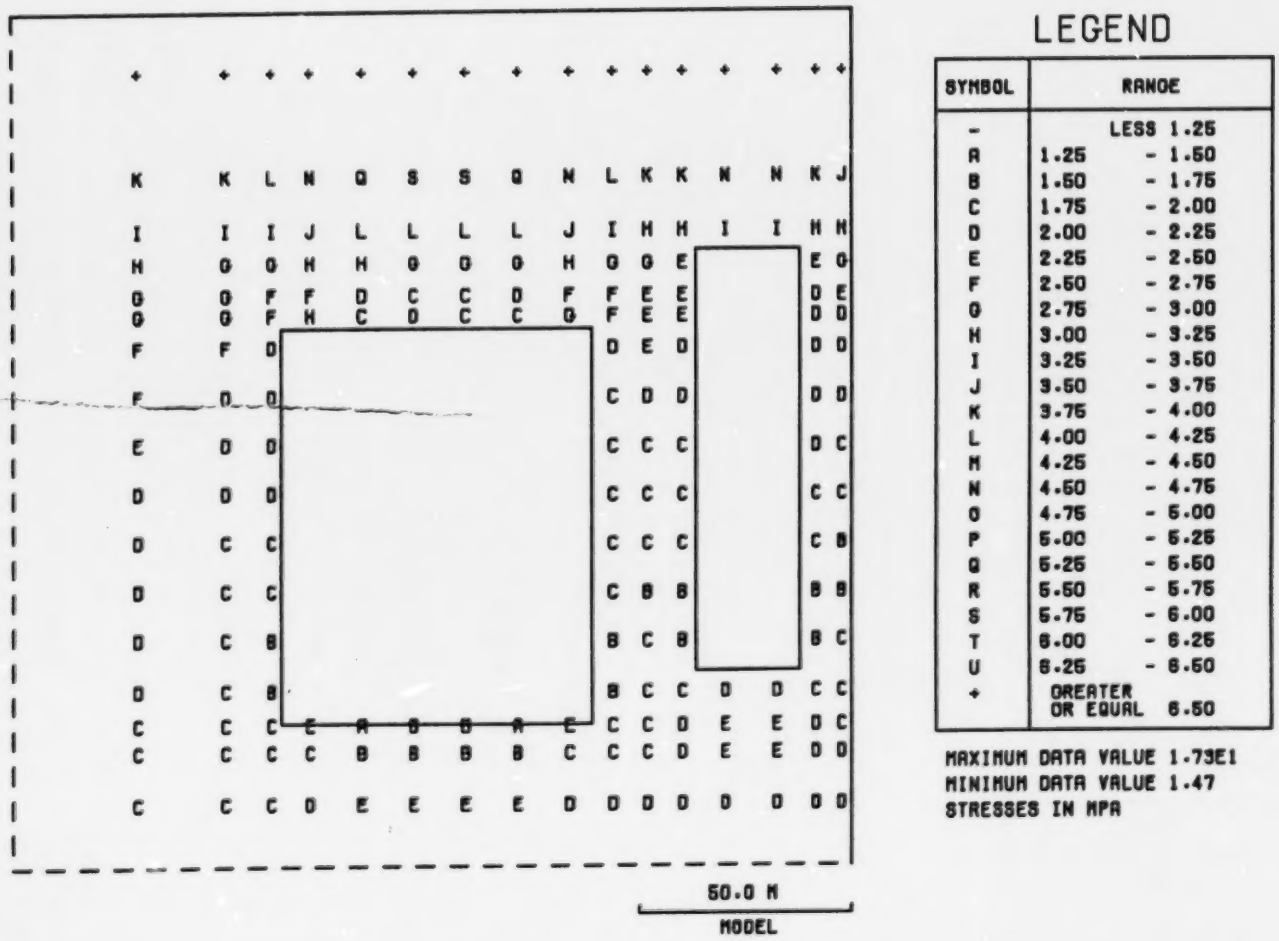

Fig. 12(a) Local Factor of Safety in Terms of Drucker/Prager Yield Function (C=1 MPa; $\phi = 40°$), Under Loading A, for Section x=95.25 m.

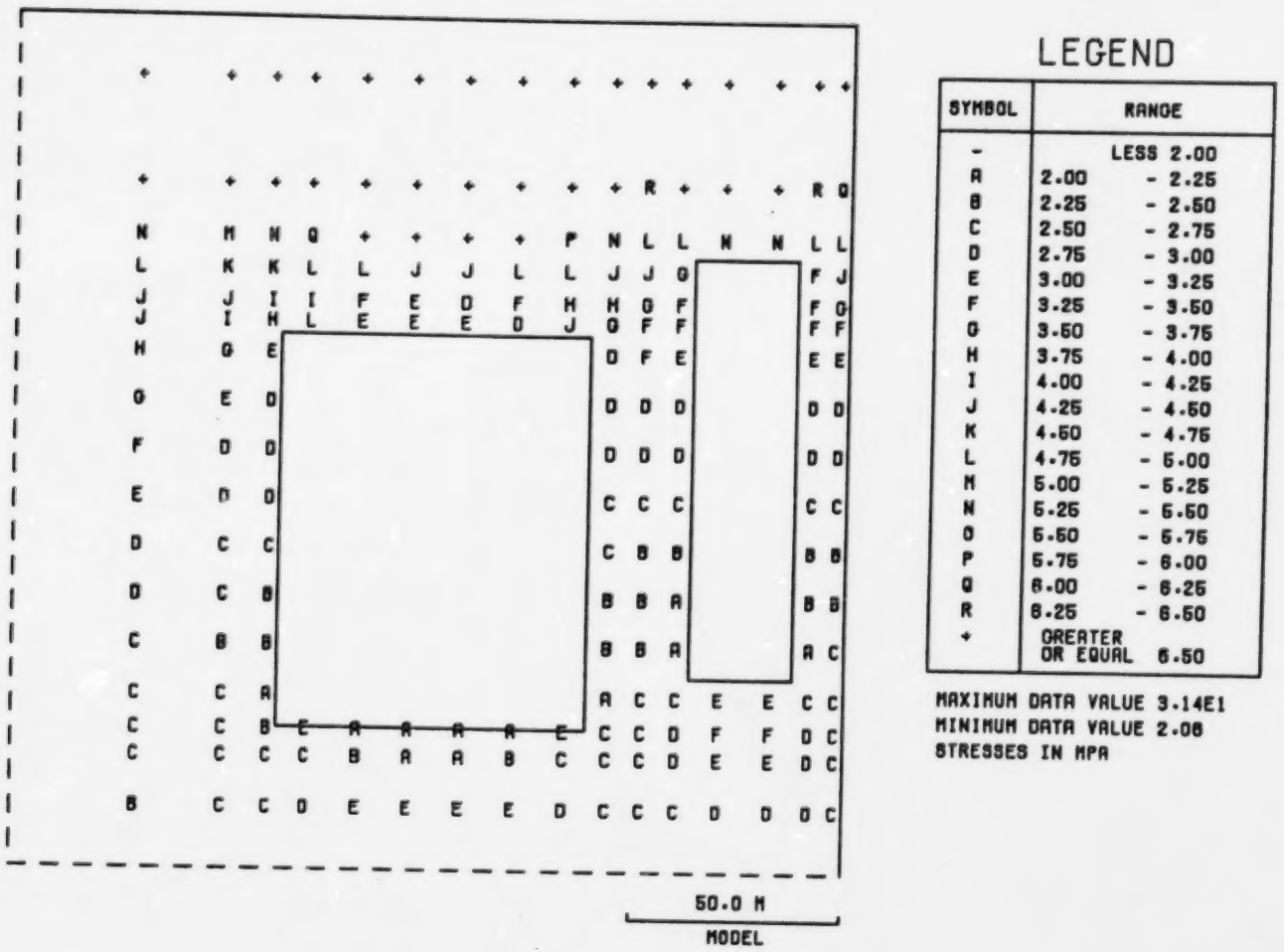

Fig. 12(b) Local Factor of Safety in Terms of Drucker/Prager Yield Function (C=2 MPa; $\phi = 40°$), Under Loading A, for Section x=95.25 m.

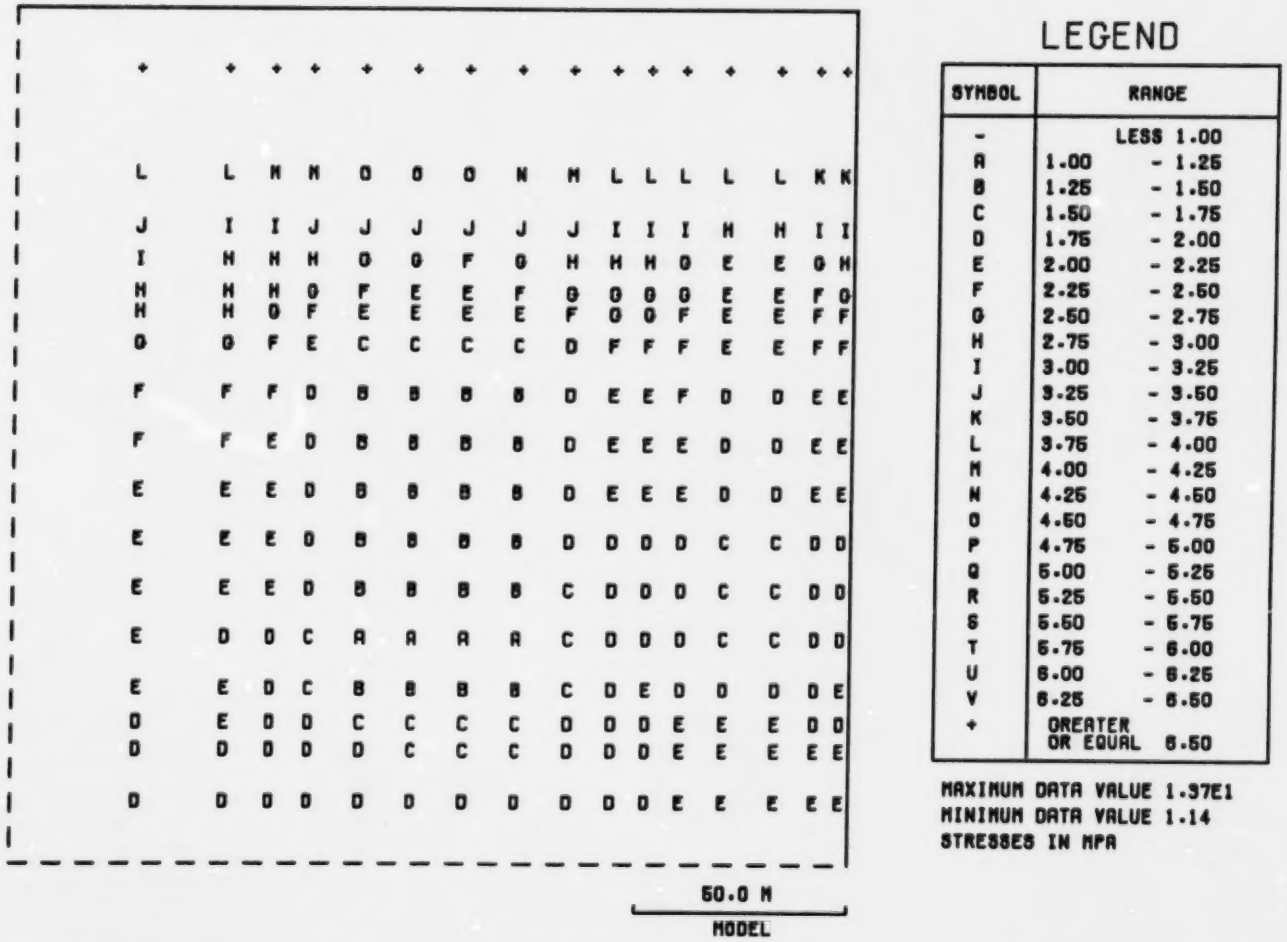

Fig. 13(a) Local Factor of Safety in Terms of Drucker/Prager Yield Function (C=1 MPa; $\phi = 40°$), Under Loading A, for Section x=88.39 m.

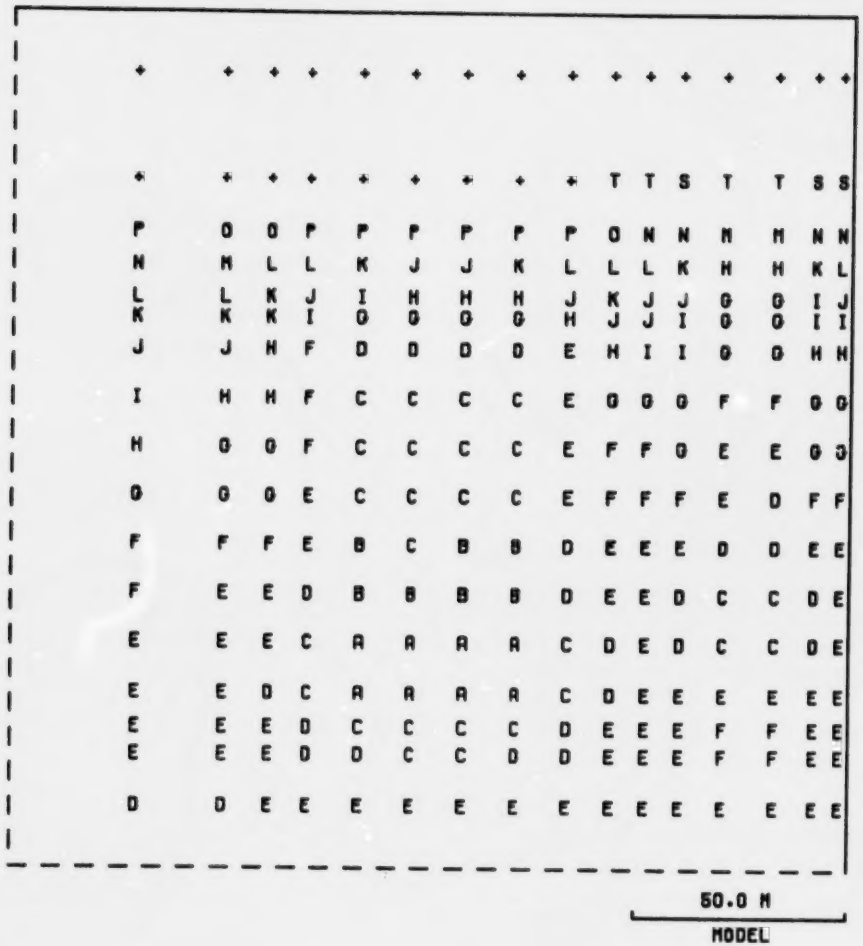
+ + + + + + + + + + + + + + + +
+ + + + + + + + + T T S T T S S
P O O P P P P P P O N N M M N N
N M L L K J J K L L L K H H K L
L L K J I H H H J K J J G G I J
K K K I G G G G H J J I G G I I
J J H F D D D D E H I I G G H H
I H H F C C C C E G G G F F G G
H G G F C C C C E F F G E E G G
G G G E C C C C E F F F E D F F
F F F E B C B B D E E E D D E E
F E E D B B B B D E E D C C D E
E E E C A A A A C D E D C C D E
E E D C A A A A C D E E E E E E
E E E D C C C C D E E E F F E E
E E E D D C C D D E E E F F E E
D D E E E E E E E E E E E E E E
50.0 M
MODEL

LEGEND

SYMBOL	RANGE
-	LESS 1.50
A	1.50 - 1.75
B	1.75 - 2.00
C	2.00 - 2.25
D	2.25 - 2.50
E	2.50 - 2.75
F	2.75 - 3.00
G	3.00 - 3.25
H	3.25 - 3.50
I	3.50 - 3.75
J	3.75 - 4.00
K	4.00 - 4.25
L	4.25 - 4.50
M	4.50 - 4.75
N	4.75 - 5.00
O	5.00 - 5.25
P	5.25 - 5.50
Q	5.50 - 5.75
R	5.75 - 6.00
S	6.00 - 6.25
T	6.25 - 6.50
+	GREATER OR EQUAL 6.50

MAXIMUM DATA VALUE 2.48E1
MINIMUM DATA VALUE 1.62
STRESSES IN MPA

Fig. 13(b) Local Factor of Safety in Terms of Drucker/Prager Yield Function (C=2 MPa; $\phi = 40°$), Under Loading A, for Section x=88.39 m.

4.0 CONCLUSIONS AND RECOMMENDATIONS

The 3-D model was constructed before stress measurements were available for the mine. Assuming a typical gravitational load, a preliminary assessment of stress conditions around C-102-23 stope as it was mined to its full 73.15m span was carried out. The mine rocks were assumed to be homogeneous, linearly elastic and isotropic.

When field stresses and the physical properties are available, the model will be re-analyzed.

Based on the results of this study, the following conclusions are reached:

(a) The magnitudes of tensile stresses developed along the stope walls (including the footwall and hangingwall), in C-102-23 stope, are relatively small; the largest tension is less than 0.3 Mpa (45 psi). The tensile zone penetrates into the wall approximately 3m.

The tensile strength of the altered carbonatite is estimated at about 5 - 10 MPa. Therefore, if no joints are unfavourably oriented in relation to the tensile stresses, the wall should be stable.

(b) Small tensions ($\leq$ 0.25 MPa) were also observed along almost the entire height of T-102-21 pillar. Since the pillar is only 24m (80 ft) wide, precautions should be taken to ensure its integrity.

(c) A large tensile zone (with magnitudes ranging from 0-0.75 MPa) was developed in the central portion of the roof in the C-102-23 stope, as shown in Figs. 8 to 9. This tensile zone extends into the centre of the roof approximately 10m (33 ft), and extends more than 10m towards both the hanging and foot walls. The largest tension ($\leq$ 0.75 MPa) occurs at the quarter span and diminishes gradually toward the walls. The ground at the quarter span of the stope back is in a state of tension as both the major and minor principal stresses are tensile. Cracks may initiate at such locations, and may propagate throughout the tensile zone. With the combination of these tensile stresses and unfavourable discontinuities, caving is anticipated.

The roof of C-102-23 stope is basically in carbonatite. Due to the large depth of the tensile zone, conventional rock bolting to strengthening the roof may not be effective. Cable bolting is recommended. It is also recommended that mining of C-102-23 stope proceeds in stages from right (east direction) to left. Continuous observations should be conducted as mining progresses in this area. If severe ground conditions develop, additional pillars should be considered.

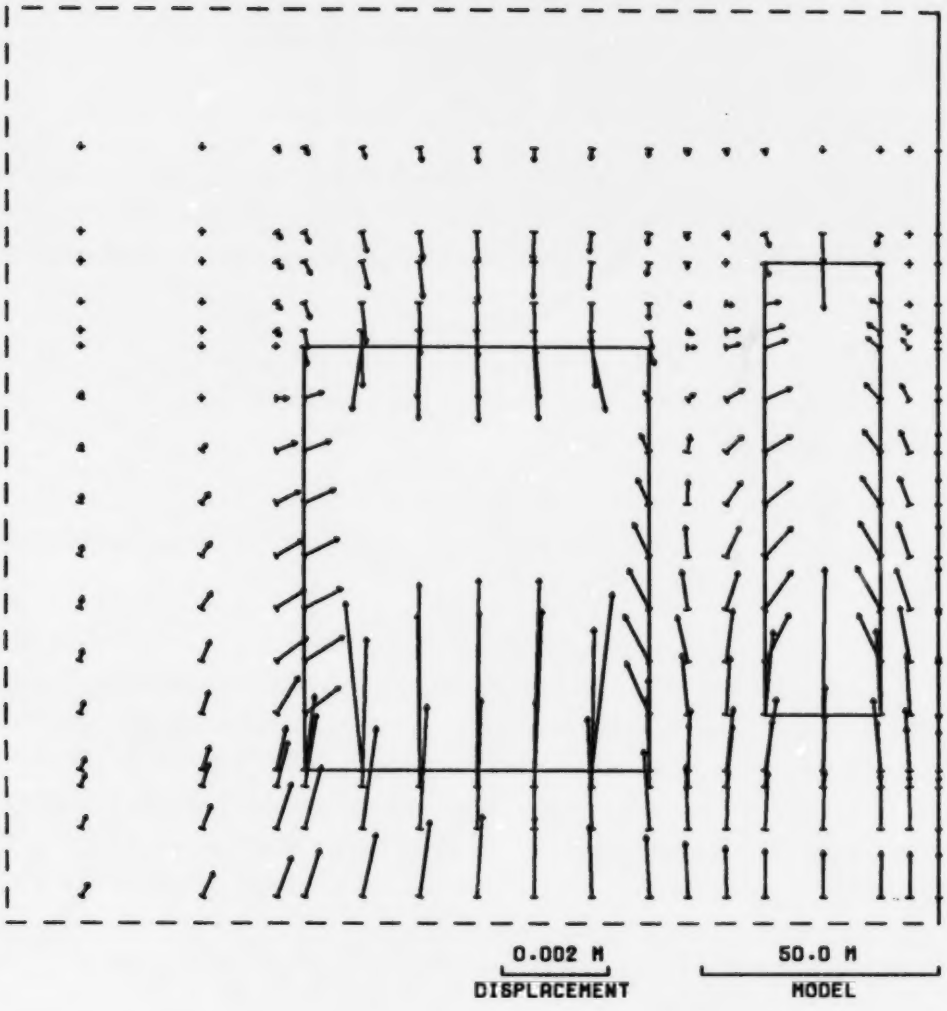

Fig. 14(a) In-plane Displacements, Under Loading A, for Section x=106.68 m.

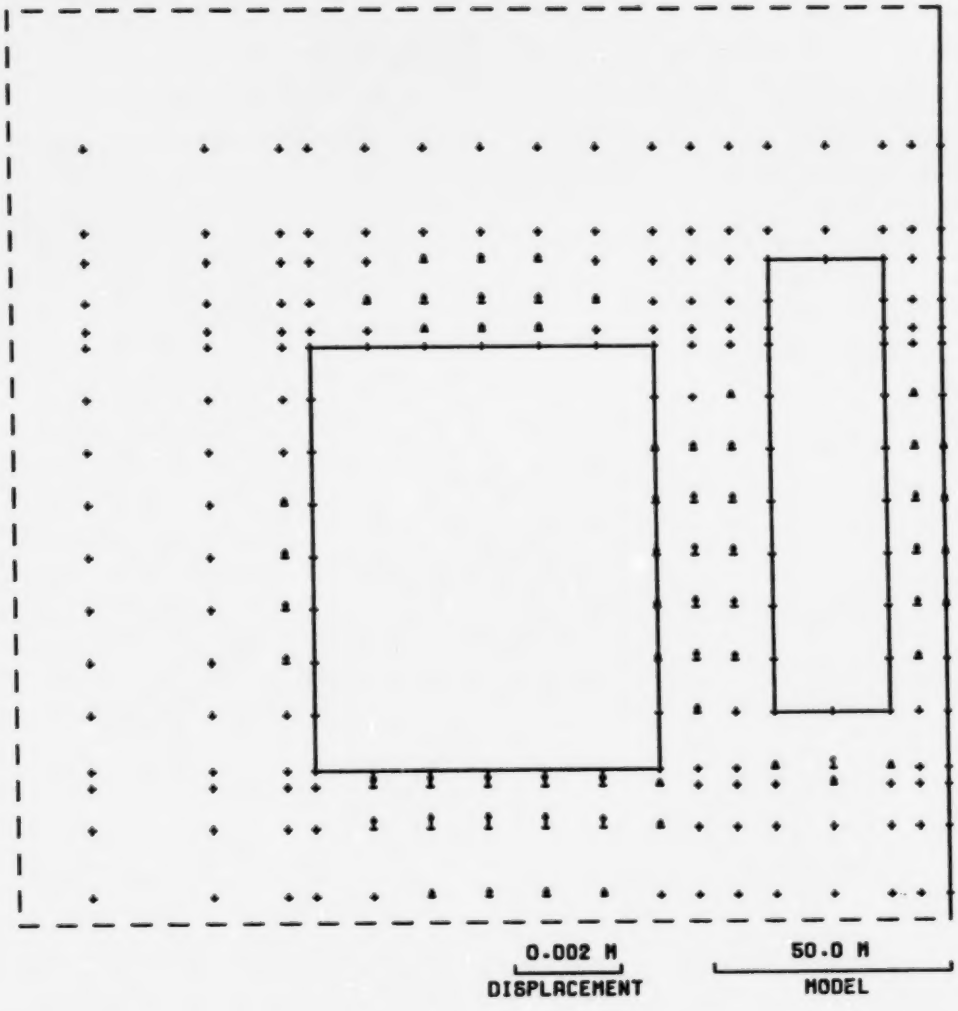

Fig. 14(b) Out-of-plane Displacements, Under Loading A, for Section x=106.68 m.

(d) It is interesting to note that large tensions (approximately 1 MPa) occur along the floor of C-102-23 stope. Floor heaving is expected.

(e) The local factor of safety calculated based on the Drucker/Prager yield criterion provides some insight in terms of shear failure. The factors calculated for the pillars range from 1.28 to 2.5 for C = 1 MPa and $\phi = 40°$. These factors were increased to 1.77 - 4.00 when C was changed to 2 MPa. A value of 2 MPa for cohesion is considered to be conservative. For long term stability (more than two years life) a factor of safety of 1.6 or greater is usually recommended. Therefore, no imminent shear failure is anticipated. If failure occurs, it would be tension failure rather than shear failure.

(f) The displacements calculated are small, and there is no real concern with these elastic displacements. If floor heaving occurs, the measured changes in elevation will be greater than predicted. This is because part of the floor will be in a state of plasticity or yield condition.

5.0 ACKNOWLEDGEMENTS

Mr. Marc Bétournay acted as liaison officer between the Niobec Mine, Centre de Recherches Minérales, Quebec, and the Mining Research Laboratories of CANMET, his effort in providing information and maintaining good communication is appreciated. The authors wish to thank MRL management for their encouragement and support.

6.0 REFERENCES

1. Gagnon, G. and Gendron, L.A.; "The geology and current development of the St. Honoré niobium (columbium) deposits"; Paper presented at the 79th Annual General Meeting of C.I.M.; 1977.

2. Wilson, E.L.; "SOLID SAP - A static analysis program for three dimensional solid structures"; University of California, Berkeley, California; Sept. 1971 (Revised March 1972).

3. Zienkiewicz, O.C.; "The finite element method in engineering science"; McGraw-Hill, London; 2nd Ed.; 1971.

4. Toews, N.A., Yu, Y.S. and Granz, R.; "Documentation of GEN3D (A 3-D Mesh Generating Program for SAP3D)"; Report MRP/MRL 75-89 (TR); Mining Research Laboratories, CANMET, Energy, Mines and Resources Canada; December, 1975.

APPENDIX A

Local Factor of Safety

The local factor of safety is calculated based on the Drucker/Prager yield function. Adopting the typical continuum mechanics sign convention (tensile stress positive), the function is written:

$$F = \alpha I_1 + \sqrt{J_2} = k$$

where I_1 = first invariant of stress tensor

$$= \frac{1}{3}(\sigma_x + \sigma_y + \sigma_z)$$

J_2 = second invariant of deviatoric stress tensor

$$= \frac{1}{6}\left[(\sigma_x - \sigma_y)^2 + (\sigma_y - \sigma_z)^2 + (\sigma_z - \sigma_x)^2 + 6(\tau_{xy}^2 + \tau_{yz}^2 + \tau_{zx}^2)\right]$$

α = material constant

$$= \frac{2\sin\phi}{\sqrt{3}(3 - \sin\phi)}$$

k = material constant

$$= \frac{6\cos\phi}{\sqrt{3}(3 - \sin\phi)}$$

where C is the cohesion and ϕ the angle of internal friction.

Factor of safety is defined to be the ratio of strength available to the strength mobilized. The stresses for each element are known from the finite element analysis, therefore, the factor of safety in terms of I_1 and J_2, and the material constants can be expressed as:

$$F_s = \frac{k - \alpha I_1}{\sqrt{J_2}}$$

The above equation can be used to calculate the factor of safety for each element and it is referred to as the local factor of safety. An element becomes plastic or yield when $F_s \leq 1.0$. $F_S > 1.0$ indicates elastic behaviour.